The influence of non-locality on fluctuation effects for 3D short-ranged wetting

2008 J. Phys.: Condens. Matter 20 505102

(http://iopscience.iop.org/0953-8984/20/50/505102)

J. Phys.: Condens. Matter **20** (2008) 505102 (22pp) doi:10.1088/0953-8984/20/50/505102

The influence of non-locality on fluctuation effects for 3D short-ranged wetting

A O Parry[1], J M Romero-Enrique[2], N R Bernardino[1,3] and C Rascón[4]

[1] Department of Mathematics, Imperial College London, London SW7 2BZ, UK
[2] Departamento de Física Atómica, Molecular y Nuclear, Universidad de Sevilla, Apartado de Correos 1065, 41080 Seville, Spain
[3] Max-Planck-Institut fur Metallforschung, 70569 Stuttgart, Germany
[4] Grupo Interdisciplinar de Sistemas Complejos (GISC), Departamento de Matemáticas, Universidad Carlos III de Madrid, 28911 Leganés, Spain

Received 4 September 2008
Published 7 November 2008
Online at stacks.iop.org/JPhysCM/20/505102

Abstract
We use a non-local interfacial Hamiltonian to revisit a number of problems associated with the fluctuation theory of critical wetting transitions in three-dimensional systems with short-ranged forces. These centre around previous renormalization group predictions of strongly non-universal critical singularities and also possible fluctuation-induced first-order (stiffness-instability) behaviour, based on local interfacial models, which are not supported by extensive Monte Carlo simulations of wetting in the three-dimensional Ising model. Non-locality gives rise to long-ranged two-body interfacial interactions controlling the repulsion from the wall not modelled correctly in previous interfacial descriptions. In particular, correlation functions are characterized by two diverging parallel correlation lengths, $\xi_\parallel$ and $\xi_{\rm NL} \propto \sqrt{\ln \xi_\parallel}$, not one as previously thought. Mean-field, Ginzburg criterion and linear renormalization group analyses all show that some interfacial fluctuation effects are strongly damped for wavenumbers $q > 1/\xi_{\rm NL}$. This prevents a stiffness-instability and reduces the size of the asymptotic critical regime where non-universality can be observed. Non-universal critical singularities along the critical wetting isotherm are determined by a smaller, effective value of the wetting parameter which slowly approaches its asymptotic limit as the wetting film grows. This is confirmed by numerical simulation of a discretized version of the non-local model.

(Some figures in this article are in colour only in the electronic version)

1. The problems of critical wetting

A long-standing puzzle within the renormalization group (RG) theory of critical phenomena concerns the nature of fluctuation effects for critical wetting transitions in three-dimensional systems with short-ranged forces [1]. The initial theoretical interest in this problem stems from the fact that the physical dimension $d = 3$ is also the upper critical dimension for the transition. RG analyses of a simple interfacial (capillary-wave) Hamiltonian by Brezin, Halperin and Leibler [2] and later Fisher and Huse [3] predict that all critical properties are strongly non-universal and depend on the dimensionless wetting parameter (see also [4])

$$\omega = \frac{k_{\rm B} T \kappa^2}{4\pi \Sigma}. \tag{1}$$

Here, Σ is the stiffness of the $\alpha\beta$ interface that unbinds continuously from an inert wall on approaching the wetting temperature $T_{\rm w}$, while $\kappa = 1/\xi_\beta$ is the inverse (true) correlation length of the bulk phase, β, that intrudes between the wall and bulk phase, α. Non-universality is predicted for the divergence of three characteristic length-scales; the equilibrium film thickness, $\langle \ell \rangle$, the interfacial roughness, $\xi_\perp$, and the parallel correlation length $\xi_\parallel$. In particular, the exponent $\nu_\parallel$ describing the divergence $\xi_\parallel \sim (T_{\rm w} - T)^{-\nu_\parallel}$ shows the highly sensitive dependence

$$\nu_\parallel(\omega) = \begin{cases} (1-\omega)^{-1} & \text{for } 0 < \omega < 1/2 \\ (\sqrt{2} - \sqrt{\omega})^{-2} & \text{for } 1/2 < \omega < 2. \end{cases} \tag{2}$$

For $\omega > 2$, the correlation length diverges exponentially quickly. This reveals a dramatic alteration to the mean-field result, $\nu_{\parallel}^{\mathrm{MF}} = 1$ [5, 6], which is only recovered for an infinitely stiff interface.

The natural testing ground for these predictions is the wetting transition in the semi-infinite simple cubic Ising model, above its roughening temperature. It is known that the wetting parameter tends to a universal value $\omega \approx 0.8$ on approaching the bulk critical temperature T_{c} [7, 8] suggesting that $\nu_{\parallel}^{\mathrm{RG}} \approx 3.7$, strikingly different from its mean-field value. As is well known, however, these predictions are not supported by extensive Monte Carlo simulation studies of wetting in the Ising model due to Binder, Landau and coworkers [9–12]. These simulations confirm the qualitative structure of the global surface phase diagram, showing the locations of first-order, critical and tricritical wetting, as predicted by Nakanishi and Fisher [6]. However, quantitative analysis of the critical singularities at critical wetting as manifest in the surface magnetization and susceptibility were found to be broadly consistent with mean-field theory. Subsequent re-analysis of the behaviour of the surface layer susceptibility near T_{w} did reveal some non-classical fluctuation effects but these are consistent with a much smaller, effective value of the wetting parameter $\omega_{\mathrm{fit}} \approx 0.28 \pm 0.12$ lying somewhere between the RG and mean-field predictions [13].

Unfortunately, the problems of critical wetting do not end here. In a series of articles in the early 1990s Fisher and Jin [14–18] addressed the above controversy and first sought to precise the derivation of an interfacial model from a more microscopic Landau–Ginzburg–Wilson (LGW) Hamiltonian by integrating out non-interfacial degrees of freedom. After clarifying this procedure, they evaluated the interfacial model as a gradient expansion in the interfacial height and showed that the original capillary-wave model must be modified to include a specific position-dependent stiffness. Then, they generalized the linear RG flow equations and showed that the new position-dependent term in the stiffness drove the bare (mean-field) critical wetting transition first-order. This stiffness-instability mechanism was forwarded as the likely explanation for the findings of the Ising model simulations.

However, there are two problems with the Fisher–Jin proposal, the second of which is very worrying. Firstly, the stiffness-instability mechanism is certainly not a quantitative explanation of the near mean-field-like criticality observed for the Ising model. Indeed, there is no explicit evidence for (weakly) first-order wetting in the simulation studies. Secondly, and more importantly, Fisher and Jin drew only one half of the conclusions predicted by their theory. If the bare critical wetting transition is driven first-order, an identical line of reasoning dictates that the bare first-order wetting transition is fluctuation-induced second-order [19]. Thus the stiffness-instability mechanism, if present in microscopic models, would serve to exchange the lines of first-order and critical wetting appearing in the equilibrium global surface phase diagram. Put more starkly, if Fisher and Jin are correct then Nakanishi and Fisher [6] must be wrong. This is an extremely unlikely scenario, not supported by the Ising simulations, which would contradict much of our understanding of wetting and surface criticality. We are thus forced to conclude, that despite its apparent systematic basis, the Fisher–Jin analysis must be incorrect. This is also true of slightly generalized versions of their model developed by one of us [20, 21], which allow for coupling between fluctuations near the interface and wall. These also show a stiffness-instability and therefore must be similarly flawed. The analysis of Fisher and Jin leaves us with a profound difficulty: if the derivation of an interfacial Hamiltonian with a position-dependent stiffness and subsequent RG analysis are sound, why does not a stiffness-instability actually occur?

In the present paper, we show how progress may be made towards resolving these and other problems using a non-local (NL) interfacial Hamiltonian. The derivation of this model, from an underlying LGW description of the wall-α interface, was described at length in our two earlier articles [22, 23]. Our original motivation was just to derive the form of the interfacial Hamiltonian for fluid adsorption near structured surfaces, in particular (acute) wedges and apexes with the prospect of understanding connections between wedge filling and wetting transitions [24–28]. Thus, the starting point of the analysis is similar to that of Fisher and Jin, but generalized to non-planar walls and identifies the interfacial Hamiltonian via a partial trace over non-interfacial-like degrees of freedom. The essential difference with the Fisher–Jin analysis is that the resulting constrained minimization problem is solved using a Green's function method, similar to multiple reflection expansion techniques employed for other problems [29–31], and does not invoke a gradient expansion. This treats the constraints arising from the interface and wall on an equal footing and reveals a general diagrammatic structure to the interfacial Hamiltonian. For example, at bulk coexistence, the binding potential functional describing the interaction between the interface and wall can be written

$W[\ell, \psi] = a$ 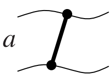 $+ b_1$ 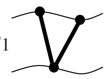 $+ \cdots$ (3)

where the upper (lower) wavy-line denotes the interface shape $\ell(\mathbf{x})$ (wall shape $\psi(\mathbf{x})$) and the straight line represents a kernel, similar to the bulk correlation function. This non-local formulation sheds new light on the problems of critical wetting discussed above. The Fisher–Jin model is only a small-gradient approximation to the NL theory which, even for planar walls, now crucially includes two-body, and indeed many-body, interfacial interactions. These are characterized by a new length-scale ξ_{NL} which diverges at the wetting transition and is intermediate between the usual parallel correlation length $\xi_{\parallel}$ and the bulk correlation length ξ_{β}. The role played by this length-scale, in particular the dampening effect it has on fluctuations, has not been appreciated previously and appears to be key to resolving several issues in the theory of wetting. While the RG theory plays a significant part in our discussion, most of the new physics can be understood simply from the structure of the two-body interfacial interaction and mean-field correlation functions. Preliminary accounts of some of our results can be found in [32] and [33].

Of necessity, our paper is quite long, dealing in turn with several aspects of the critical wetting story in some depth. The material covered in the remaining sections is as follows.

Section 2. *Three interfacial Hamiltonians*. We compare and contrast the capillary-wave (CW), Fisher–Jin (FJ) and NL interfacial models recalling the linear RG analysis of the first two. The nature of the two-body interfacial repulsion in the NL model is discussed and the CW and FJ models are recovered as long-wavelength approximations. The FJ model is shown to get the sign of the interaction wrong for wavenumbers $q > 1/\xi_{NL}$ and is strongly suggestive that the predicted stiffness-instability is an artefact of a poor long-wavelength approximation.

Section 3. *Mean-field correlations revisited*. We show that the presence of long-ranged two-body interfacial interactions can be seen explicitly in the mean-field pair-wise correlation function $G(\mathbf{r}_1, \mathbf{r}_2)$ calculated using the underlying LGW theory. A closed form expression for $G(\mathbf{r}_1, \mathbf{r}_2)$, or rather its parallel Fourier transform $\mathcal{G}(z_1, z_2; q)$, is found by solving the Ornstein–Zernike equation. This is characterized by two parallel correlation lengths, $\xi_\parallel$ and $\xi_{NL} \propto \sqrt{\ln \xi_\parallel}$, signifying a breakdown of simple scaling. In general, the second length-scale dampens and cuts-off interfacial fluctuation effects with wavenumbers $q > 1/\xi_{NL}$. We also show that within the NL theory there exists a simple diagrammatic representation and visualization of microscopic (spin–spin or density–density) correlations, similar to (3), arising from the coupling of tube-like fluctuations with the capillary-wave modes of the unbinding interface. The singular contribution to G may be written

$$G^{\mathrm{sing}}(\mathbf{r}_1, \mathbf{r}_2) \propto \frac{\partial^2}{\partial z_1 \partial z_2} \qquad (4)$$

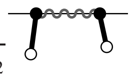

where the wiggly line represents the height–height correlation and the open circles denote the points $\mathbf{r}_1$ and $\mathbf{r}_2$. This recovers the expression for the singular contribution to G calculated using the LGW model. We point out that the NL theory is thermodynamically consistent and satisfies an exact sum-rule requirement for complete wetting due to Henderson [34], which is not fully obeyed by the capillary-wave theory [35, 36].

Section 4. *The Ginzburg criterion revisited*. Our final sections deal with fluctuation effects beyond mean-field beginning with a discussion of the modification of the Ginzburg criterion determining the size of the asymptotic critical regime. This is reduced within the NL theory due to the length-scale ξ_{NL}, which serves to cut-off part of the capillary-wave spectrum, and highlights the role played by an effective wetting parameter. This effect can be traced directly to the structure of the mean-field correlation function and, by implication, the two-body interfacial repulsion.

Section 5. *Linear RG analysis*. The linear RG analysis of Fisher and Huse is generalized to account for a two-body interfacial interaction. Five things follow (1) No stiffness-instability at critical wetting can occur because the two-body interaction is always repulsive. (2) The renormalized repulsion from the wall is weaker than predicted by the CW theory. (3) Mean-field-like critical exponents play a more prominent role as a lower bound on the critical behaviour, even in the presence of fluctuations effects. (4) The leading-order asymptotic critical behaviour displays the same non-universality predicted by the CW theory but in a narrower critical regime. (5) The renormalized repulsion is controlled by an effective wetting parameter, similar to that emerging from the Ginzburg criterion, which only approaches its limiting value rather slowly as the wetting film grows. It is this reduced effective wetting parameter which determines the critical singularities occurring along the critical wetting isotherm.

All these effects can be viewed as arising because the momentum cut-off appearing in the original CW description of the interfacial repulsion should be replaced with a lower, effective, value $\Lambda_{NL} \approx 1/\xi_{NL}$ which cuts-off part of the capillary-wave spectrum interacting with the wall.

Section 6. *Simulation studies*. Simulation studies of discretized versions of the CW, FJ and NL models are reported. These support the predictions based on the respective linear RG analyses for each of these models. For the NL model the approach to the critical regime is slower than for the CW model and we extract, numerically, the effective value of the wetting parameter as a function of film thickness. This is compared with theoretical predictions and the fitted value ω_{fit} obtained from the Ising model simulations [13].

2. Three interfacial Hamiltonians

2.1. The capillary-wave model

In three dimensions, microscopic studies of wetting are limited to mean-field models such as Landau, square-gradient theory and other approximate density-functional descriptions which neglect large-scale fluctuation effects [1, 5, 6, 37, 38]. To predict the latter, it has been necessary to resort to effective Hamiltonian models based on a collective coordinate $\ell(\mathbf{x})$ measuring the local interfacial height at vector position $\mathbf{x} = (x, y)$ above the wall (see figure 1). The original model proposed for three-dimensional wetting was [2]

$$H_{CW}[\ell] = \int \mathrm{d}\mathbf{x} \left\{ \frac{\Sigma}{2} (\nabla \ell)^2 + W(\ell) \right\} \qquad (5)$$

where, for isotropic fluids or continuum models (such as the LGW theory), we may identify the stiffness Σ with the free interfacial tension $\sigma_{\alpha\beta}$ [39]. We refer to this as the capillary-wave model. Interfacial models are only appropriate descriptions of microscopic fluctuations at sufficiently long-wavelength fluctuations and the first term in the CW model, describing the energy cost of increasing the area of the interface is only valid for the wavenumbers $0 \leqslant q < \Lambda$ where $\Lambda \approx \kappa$ is the high momentum cut-off. The assumption of all previous effective Hamiltonian studies of wetting is that this cut-off is also appropriate for the binding potential describing the wall–interface interaction. This binding potential was taken to have the form

$$W(\ell) = \bar{h}\ell + a\mathrm{e}^{-\kappa\ell} + b_1 \mathrm{e}^{-2\kappa\ell} + \cdots \qquad (6)$$

together with a hard-wall repulsion restricting the collective coordinate $\ell(\mathbf{x}) > 0$. Formally, $W(\ell)$ can be identified as the free-energy of a planar interfacial configuration which is constrained to be at a (uniform) height ℓ above the wall. The field $\bar{h}$ measures the deviation from two-phase coexistence and, in magnetic language, is proportional to the bulk ordering

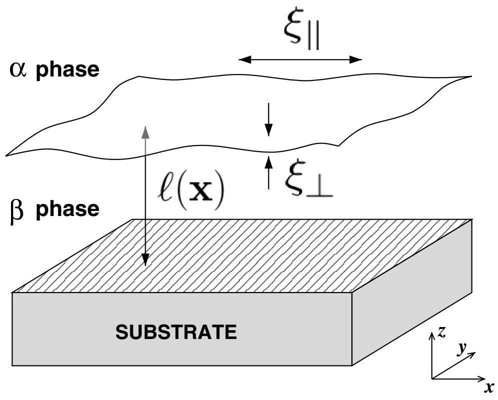

Figure 1. Schematic illustration of a wetting layer of phase β at the interface between a planar substrate and bulk α phase. A collective coordinate $\ell(\mathbf{x})$ describes the local height of the $\alpha\beta$ interface above the substrate. Fluctuations of the unbinding interface are characterized by perpendicular ($\xi_\perp$) and parallel ($\xi_\parallel$) correlation lengths.

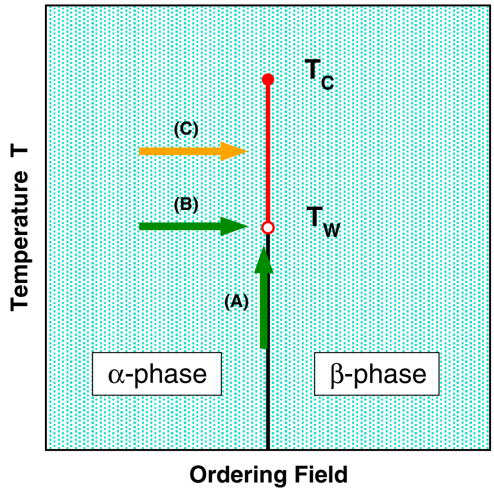

Figure 2. Phase diagram showing the coexistence between phases α and β, represented by the black line ending at T_c. The substrate is wet by phase β above T_w, at any point of the red segment. Different surface phase transitions are represented by the arrows: critical wetting (paths A and B) and complete wetting (path C).

field. The coefficient $a \propto T - T_w^{MF}$ changes sign at the bare (mean-field) critical wetting temperature T_w^{MF} while the second coefficient $b_1 > 0$ is a constant. Here, we have placed a subscript on the coefficient of the repulsion to distinguish it from the spacial rescaling factor in the RG analysis and also to make connection with the Fisher–Jin and NL theories easier.

A section of the global surface phase diagram showing critical and complete wetting transitions is shown in figure 2. Critical wetting refers to the continuous divergence of the film thickness as $T \to T_w$ and $\bar{h} \to 0^+$ for which one usually focuses on the two representative thermodynamic paths shown as (A) and (B). Complete wetting (path C) on the other hand, refers to the approach to coexistence above the wetting temperature and is described by a different set of critical exponents. These will be introduced when necessary. On approaching a wetting transition, the singular contribution to the surface tension, defined as

$$\sigma_{\text{sing}} = \sigma_{w\alpha} - \sigma_{w\beta} - \sigma_{\alpha\beta} \tag{7}$$

vanishes, equivalent to having zero contact angle. Here $\sigma_{w\alpha}$ denotes the surface tension of the wall-α interface, etc.

Before we consider the RG method we mention, that if fluctuations are ignored and $H_{CW}[\ell]$ is simply minimized, the mean-field expression for the film thickness, $\hat{\ell}$, is recovered from solution of $W'(\hat{\ell}) = 0$ and determines the singular contribution to the excess free-energy per unit area $\sigma_{\text{sing}} = W(\hat{\ell})$. Similarly, if one considers small, Gaussian, fluctuations about the height $\hat{\ell}$, we may determine the mean-field expression for the height–height correlation function. The Fourier transform of this is defined as

$$g(q) \equiv \int d\mathbf{x}_{12}\, \langle \delta\ell(\mathbf{x}_1)\delta\ell(\mathbf{x}_2)\rangle e^{i\mathbf{q}\cdot\mathbf{x}_{12}} \tag{8}$$

where $\delta\ell(\mathbf{x}) = \ell(\mathbf{x}) - \hat{\ell}$. For the CW model, the mean-field expression for $g(q)$ follows directly from equipartition:

$$g_{CW}(q) = \frac{k_B T}{W''(\hat{\ell}) + \Sigma q^2} \tag{9}$$

identifying a parallel correlation length $\xi_\parallel = \sqrt{\Sigma/W''(\hat{\ell})}$. Within the CW theory, this is also the true correlation length determining the large-distance decay of the height–height correlation function. The simple Lorentzian form of the structure factor (9), characteristic of classic Ornstein–Zernike theory indicates that within the CW description there is only one diverging length parallel to the wall.

A particularly clear exposition of the RG theory of three-dimensional wetting was provided by Fisher and Huse (FH) [3] (see also the appendix in [40]). The interfacial Hamiltonian is written

$$H_{CW}[\ell] = H_0[\ell] + H_1[\ell] \tag{10}$$

where the free Hamiltonian is

$$H_0[\ell] = \int^\Lambda d\mathbf{x}\, \frac{\Sigma}{2}(\nabla\ell)^2. \tag{11}$$

The superscript denotes the high momentum cut-off, which restricts the Fourier space components $\tilde{\ell}(\mathbf{q})$ of $\ell(\mathbf{x})$ to wavenumbers $q < \Lambda$. The interaction of the interface with the wall is described by the local functional

$$H_1[\ell] = \int^\Lambda d\mathbf{x}\, W(\ell). \tag{12}$$

As explained by FH, the collective coordinate is divided into 'fast' and 'slow' contributions,

$$\ell(\mathbf{x}) = \ell_<(\mathbf{x}) + \ell_>(\mathbf{x}) \tag{13}$$

where the 'fast' part

$$\ell_>(\mathbf{x}) = \int_{\Lambda/b}^{\Lambda} d\mathbf{q}\, e^{i\mathbf{q}\cdot\mathbf{x}}\tilde{\ell}(\mathbf{q}) \tag{14}$$

contains wavenumbers in the range $\Lambda/b < q < \Lambda$. Here $b = e^t$ is the spacial rescaling factor, so that $\mathbf{x}' = \mathbf{x}/b$, while t is the infinitesimal renormalization parameter. In general dimension d, the collective coordinate transforms as $\ell(\mathbf{x}') = b^{(d-3)/2}\ell(\mathbf{x})$ so that the free Hamiltonian (11) is a non-trivial fixed-point of the RG transformation. Specializing to three dimensions ($d = 3$), FH show that a linear functional RG analysis leads to the partial differential equation

$$\frac{\partial W_t}{\partial t} = 2W_t + \omega\xi_\beta^2\frac{\partial^2 W_t}{\partial \ell^2} \tag{15}$$

describing the flow of the renormalized binding potential $W_t(\ell)$. This is solved by

$$W_t(\ell) = \frac{\kappa\,\mathrm{e}^{2t}}{\sqrt{4\pi\omega t}}\int_{-\infty}^{\infty}\mathrm{d}\ell'\; W_0(\ell')\,\mathrm{e}^{-\kappa^2(\ell-\ell')^2/4\omega t}. \tag{16}$$

To obtain the critical singularities of the wetting transition, the RG transformation is carried through until a matching point $t = t^*$ where, at the minimum $\ell = \ell^*$ of $W_{t^*}(\ell)$, one has

$$W''_{t^*}(\ell^*) = \Sigma\Lambda^2. \tag{17}$$

This is the condition that the renormalized correlation length is the same size as the inverse momentum cut-off. At this scale, mean-field theory is valid and we can identify the original parallel correlation length

$$\Lambda\xi_\parallel = \mathrm{e}^{t^*} \tag{18}$$

and similarly for the equilibrium film thickness $\langle\ell\rangle = \ell^*$ and excess free-energy $\sigma_{\mathrm{sing}} = \mathrm{e}^{-2t^*}W_{t^*}(\ell^*)$. This flow equation is exact to linear order in the potential but does not describe properly the renormalization of the hard-wall repulsion. This is handled approximately by assuming that, for $\ell < 0$, the binding potential is a positive constant c. Thus, at $\bar{h} = 0$, the bare binding potential is taken to be

$$W_0(\ell) = W_0^{\mathrm{att}}(\ell) + W_0^{\mathrm{rep}}(\ell) + c\Theta(-\ell) \tag{19}$$

where

$$W_0^{\mathrm{att}}(\ell) = a\mathrm{e}^{-\kappa\ell}\Theta(\ell), \qquad W_0^{\mathrm{rep}}(\ell) = b_1\mathrm{e}^{-2\kappa\ell}\Theta(\ell) \tag{20}$$

and $\Theta(\ell)$ is the Heaviside step function. For reasons that will become clear later, let us focus explicitly on the renormalization of the direct repulsion within the CW theory and write

$$W_t^{\mathrm{rep}}(\ell;\omega) = \frac{b_1\kappa\,\mathrm{e}^{2t}}{\sqrt{4\pi\omega t}}\int_0^{\infty}\mathrm{d}\ell'\mathrm{e}^{-2\kappa\ell'-\kappa^2(\ell-\ell')^2/4\omega t} \tag{21}$$

where we have highlighted explicitly the dependence on the wetting parameter.

The interplay between the three contributions to $W_t(\ell)$ arising from the attractive, repulsive and hard-wall contributions leads to the three-fluctuation regimes described earlier. We will not need to repeat all these details but some remarks about regimes (I) and (II) are necessary for later reference. In regime (I), for which $0 < \omega < 1/2$ the hard-wall contribution ($\propto c$) can be dropped and the convolutions of the first-two terms in (19) are insensitive to the short-distance restriction $\ell > 0$. The renormalized potential retains its exponential form

$$W_t(\ell)\mathrm{e}^{-2t} \approx a\mathrm{e}^{\omega t-\kappa\ell} + b_1\mathrm{e}^{4\omega t-2\kappa\ell} \tag{22}$$

representing the leading-order decays. The wetting transition still occurs at the mean-field phase boundary and the matching condition determines $\xi_\parallel \sim (T_{\mathrm{w}} - T)^{-1/(1-\omega)}$ and

$$\kappa\langle\ell\rangle = (1+2\omega)\ln\xi_\parallel. \tag{23}$$

This approximation is self-consistent provided the value of ℓ' that maximizes the integrand (at the matching point), in the saddle point evaluation of (21), is greater than zero. This is valid for $\omega < 1/2$, which defines regime (I).

For $\omega > 1/2$, the analysis is more algebraically involved. In regime (II), $1/2 < \omega < 2$, the transition still occurs at $a = 0$ but now the hard-wall contribution ($\propto c$) is the same order as the renormalized repulsion ($\propto b_1$). This is because, at the matching point, the contribution to the integrand in (21) is biggest for $\ell' = 0$. The renormalized repulsion is determined by fluctuations that take the interface down to the wall. On the other hand the attractive term remains unchanged from that shown in (22). The critical exponent is now given by $\nu_\parallel = (\sqrt{2}-\sqrt{\omega})^{-2}$ and the equilibrium wetting layer thickness satisfies

$$\kappa\langle\ell\rangle = \sqrt{8\omega}\ln\xi_\parallel + \cdots. \tag{24}$$

Finally, in regime (III), $\omega > 2$, the three contributions to $W_t(\ell)$ are similar since all are dominated by the short-distance behaviour close to the wall. Analysis shows that fluctuations lower the wetting transition temperature and lead to a correlation length $\xi_\parallel$ that grows exponentially as $T \to T_{\mathrm{w}}$. Behaviour pertinent to this regime will not be our main concern.

The predictions of the linear RG theory rely on an approximate description of the hard-wall repulsion. Indeed in regimes (II) and (III), the explicit form of the renormalized hard-wall repulsion is required to determine the critical behaviour. The hard-wall is treated much better using a nonlinear functional RG scheme [41], although, unfortunately, it is no longer possible to extract analytically the ω dependence of critical quantities. However, simulations of a discretized version of the CW model [42] lend very strong support to the presence of large-scale interfacial fluctuations and the non-universality predicted by the linear RG analysis.

2.2. The Fisher–Jin model

Fisher and Jin [14–18] constructed an interfacial model systematically by means of a constrained minimization of a continuum LGW model, based on a magnetization-like order-parameter. In the small-gradient (long-wavelength) limit they showed that the interfacial model should be generalized to

$$H_{\mathrm{FJ}}[\ell] = \int\mathrm{d}\mathbf{x}\left\{\frac{\Sigma(\ell)}{2}(\nabla\ell)^2 + W(\ell)\right\} \tag{25}$$

containing a position-dependent stiffness-coefficient $\Sigma(\ell) = \Sigma + \Delta\Sigma(\ell)$. Both $W(\ell)$ and $\Delta\Sigma(\ell)$ are determined by the double-well potential appearing in the LGW model, but are robust to its precise form. Within the highly reliable double-parabola approximation (see later), the binding potential is essentially the same as the simple CW expression and, at $\bar{h} = 0$, reads

$$W(\ell) = a\mathrm{e}^{-\kappa\ell} + (b_1 + b_2)\mathrm{e}^{-2\kappa\ell} + \cdots \tag{26}$$

where $b_2 \propto a^2$ and b_1 is a positive (negative) constant for critical (first-order) wetting. The position-dependent stiffness decays as

$$\Delta\Sigma(\ell) = a\mathrm{e}^{-\kappa\ell} - 2\kappa\ell b_1\mathrm{e}^{-2\kappa\ell} + \cdots. \tag{27}$$

FJ assumed that their model was valid over the same wavenumber range as the original CW model, $0 \leqslant q < \Lambda$, and derived new RG flow equations

$$\frac{\partial W_t}{\partial t} = 2W_t(\ell) + \omega\xi_\beta^2\frac{\partial^2 W_t(\ell)}{\partial\ell^2} + \omega\xi_\beta^2\Lambda^2\Delta\Sigma_t(\ell) \tag{28}$$

$$\frac{\partial\Delta\Sigma_t(\ell)}{\partial t} = \omega\xi_\beta^2\frac{\partial^2\Delta\Sigma_t(\ell)}{\partial\ell^2} \tag{29}$$

which they de-coupled. In particular, they showed that the binding potential renormalizes precisely as in the original FH analysis (16), but as if the bare potential were modified and replaced with

$$\bar{W}_0(\ell) = W_0(\ell) + \frac{\omega\xi_\beta^2\Lambda^2}{2}(1 - \mathrm{e}^{-2t})\Delta\Sigma(\ell). \tag{30}$$

For large t, relevant to discussions of critical wetting, the t dependence can be ignored so that $\bar{W}_0(\ell)$ and $W_0(\ell)$ differ only by a fixed term determined by $\Delta\Sigma(\ell)$. Therefore, for positive $\ell > 0$, the bare modified binding potential is

$$\bar{W}_0(\ell) = \bar{a}\mathrm{e}^{-\kappa\ell} + b_1(1 - \omega\xi\ell\Lambda^2)\mathrm{e}^{-2\kappa\ell} \tag{31}$$

where $\bar{a} = (1 + \omega\xi_\beta^2\Lambda^2/2)a$. Thus, the leading-order contribution to the decay of $\Delta\Sigma(\ell)$ has a benign effect and simply rescales the coefficient a. The influence of the next-to-leading-order term is much more dramatic and raises the possibility that the mean-field critical wetting transition is driven first-order because the sign of the second term $\propto b_1$ is negative for thick wetting films. The situation is most clear-cut in regime (I), $0 < \omega < 1/2$ where the hard-wall is unimportant and a stiffness-instability must occur (within this model). The matching conditions show that the singular contribution to the free-energy, σ_{sing}, vanishes at a positive value of a when the film thickness $\langle\ell\rangle$ is finite. This corresponds to a first-order wetting transition. The situation is considerably messier for $\omega > 1/2$ when the short-distance interactions of the interface and wall are important. FJ argue that the transition is first-order for sufficiently small values of $\omega < \omega^*$ beyond which the hard-wall restores the continuous nature of the phase transition. On the basis of a linear RG analysis, they estimated that the tricritical value $\omega^* \approx 1$, and concluded that the critical wetting transition observed in the Ising model by Binder and co-workers must be (weakly) first-order. An improved treatment of the FJ model based on a numerical integration of a nonlinear RG scheme [43] showed that ω^* may be substantially larger than this estimate and supported strongly the stiffness-instability scenario for the model (25).

However, this whole line of reasoning must be mistaken in regard to the real physics. What was missing in the original interpretation was consideration of the impact on the global surface phase diagram. In particular, Fisher and Jin did not consider the converse example of a bare first-order transition ($b_1 < 0$). The same mixing of the RG flow equations implies that the transition is now fluctuation-induced second-order with similar non-universality (up to logarithmic corrections) predicted by the original CW model. Since the coefficients a and b_1 appearing in $W(\ell)$ and $\Sigma(\ell)$ are uniquely determined by the surface field and surface enhancement of the underlying LGW model this implies that the Nakanishi–Fisher global surface phase diagrams [6] are drastically altered. Specifically, if the stiffness-instability mechanism is to be believed, the loci of all lines of first-order and critical wetting have to be interchanged [19]. This scenario is quite unacceptable and is in direct conflict with the Ising model simulation studies. The Fisher–Jin theory should therefore be regarded as a paradox. We need to understand how a seemingly better interfacial Hamiltonian leads to worse predictions.

2.3. The non-local Hamiltonian

Fisher and Jin constructed their interfacial model perturbatively as a gradient expansion by considering small deviations from planar (constrained) profiles. As described in [22, 23], it is possible to do this non-perturbatively using a Green's function method closely related to multiple reflection expansion techniques [29–31]. This has a number of advantages and allows one to derive an interfacial model for wetting at non-planar walls. The NL Hamiltonian can be written

$$H_{\mathrm{NL}}[\ell,\psi] = \sigma_{\alpha\beta}A + \bar{h}V_\beta + W_{\mathrm{NL}}[\ell,\psi] \tag{32}$$

and is valid for length-scales larger than the bulk correlation length. Curvature corrections related to rigidity-like terms can be calculated but are not considered here [23]. The interfacial area is denoted $A = \int \mathrm{d}\mathbf{x}\sqrt{1 + (\nabla\ell)^2}$ while $V_\beta = \int \mathrm{d}\mathbf{x}\,(\ell(\mathbf{x}) - \psi(\mathbf{x}))$ is the volume of wetting film. The first-two terms in the model are therefore the same as those appearing in the CW model. The binding potential functional $W_{\mathrm{NL}}[\ell,\psi]$ describes the interaction of the interface and wall. Within the double-parabola approximation, it is given by

$$W_{\mathrm{NL}}[\ell,\psi] = \sum_{n=1}^{\infty}\left\{a\Omega_n^n + b_1\Omega_n^{n+1} + b_2\Omega_{n+1}^n\right\} \tag{33}$$

with geometry independent coefficients a, b_1 and $b_2 \propto a^2$ the same as in the FJ binding potential. The last class of terms (diagrams) are therefore unimportant for critical wetting provided T_{w} is not altered by fluctuations. Each of the contributions Ω_μ^ν has a diagrammatic representation in which a zig-zagging straight line (each zig and zag representing a kernel) connects μ points on the wall (lower wavy-line) to ν

points on the interface (upper wavy-line). The two dominant diagrams, with their algebraic expression, are

$$\Omega_1^1[\ell,\psi] = $$ 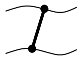 $$ = \int\int \mathrm{d}\mathbf{s}_\psi\, \mathrm{d}\mathbf{s}_\ell\, K(\mathbf{r}_\psi, \mathbf{r}_\ell) \qquad (34)$$

$$\Omega_1^2[\ell,\psi] = $$ 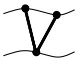 $$ = \int \mathrm{d}\mathbf{s}_\psi \left\{ \int \mathrm{d}\mathbf{s}_\ell\, K(\mathbf{r}_\psi, \mathbf{r}_\ell) \right\}^2. \qquad (35)$$

Here, $\mathbf{r}_\psi$ and $\mathbf{r}_\ell$ are points on the wall and interface respectively, which are integrated over using the appropriate infinitesimal areas $\mathrm{d}\mathbf{s}_\psi = \mathrm{d}\mathbf{x}\sqrt{1+(\nabla\psi)^2}$ and $\mathrm{d}\mathbf{s}_\ell = \mathrm{d}\mathbf{x}\sqrt{1+(\nabla\ell)^2}$. These surface integrations are implied by the black circles in the diagrams. The kernel, denoted by each straight line, is

$$K(\mathbf{r}_1,\mathbf{r}_2) = \frac{\kappa}{2\pi|\mathbf{r}_1-\mathbf{r}_2|}\mathrm{e}^{-\kappa|\mathbf{r}_1-\mathbf{r}_2|} \qquad (36)$$

and is simply a normalized version of the bulk correlation function. Thus, within the NL theory, the bare interaction between the interface and wall emerges from bulk-like fluctuations, constrained by the confining surfaces. It is tempting to view the terms in W_{NL} arising from virtual tube-like fluctuations which tunnel between the interface and wall, but this interpretation is not needed explicitly.

If both the wall and interface are planar, corresponding to a thin film of constant thickness ℓ and area A, all the diagrams reduce to $\Omega_\nu^\mu = A\mathrm{e}^{-n\kappa\ell}$, where n is simply the number of kernels (straight-lines) that span the surfaces. In this case we recover the full expression for the FJ binding potential function (in zero bulk field) $W(\ell) \equiv W[\ell]/A$:

$$W(\ell) = \frac{a\mathrm{e}^{-\kappa\ell} + (b_1+b_2)\mathrm{e}^{-2\kappa\ell}}{1-\mathrm{e}^{-2\kappa\ell}} \qquad (37)$$

which shows a hard-wall divergence as $\ell \to 0$.

Specializing to the case of wetting at a planar wall, the NL Hamiltonian reduces to

$$H_{\mathrm{NL}}[\ell] = \int \mathrm{d}\mathbf{x} \left\{ \frac{\Sigma}{2}(\nabla\ell)^2 + \bar{h}\ell \right\} + W_{\mathrm{NL}}[\ell] \qquad (38)$$

where we have taken the usual gradient expansion for the bending term, and dropped a constant contribution. Recall the stiffness and tension are the same for the isotropic LGW model. The binding potential functional may be taken as

$$W_{\mathrm{NL}}[\ell] = a$$ 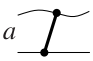 $$+\, b_1$$ 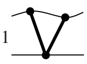 $$+\cdots \qquad (39)$$

containing just the two most important diagrams. The first diagram reduces to

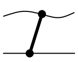 $$= \int \mathrm{d}\mathbf{s}\, \mathrm{e}^{-\kappa\ell} \qquad (40)$$

where $\mathrm{d}\mathbf{s} = \sqrt{1+(\nabla\ell)^2}\mathrm{d}\mathbf{x}$. This contribution is very similar to terms appearing in simpler CW and FJ models. This is also true for the (irrelevant) diagram $\Omega_2^1 = \int \mathrm{d}\mathbf{s}\, \mathrm{e}^{-2\kappa\ell}$ which is also local and generates the $b_2\mathrm{e}^{-2\kappa\ell}$ term in (26).

Differences between the CW and FJ models emerge from the Ω_1^2 diagram, describing the direct repulsion at critical wetting. Using a convolution to integrate over the point on the wall leads to

$$b_1$$ 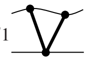 $$= \int\int \mathrm{d}\mathbf{s}_1\, \mathrm{d}\mathbf{s}_2 U(x_{12};\bar{\ell}) \qquad (41)$$

where $\mathrm{d}\mathbf{s}_i = \mathrm{d}\mathbf{x}_i\sqrt{1+(\nabla\ell(\mathbf{x}_i))^2}$ is the infinitesimal interfacial area at the points ($i = 1, 2$) and

$$U(x;\ell) = \frac{b_1\kappa^2}{2\pi}\int_{2\kappa\ell}^{\infty} \mathrm{d}\tau \frac{\mathrm{e}^{-\sqrt{\tau^2+\kappa^2x^2}}}{\sqrt{\tau^2+\kappa^2x^2}} \qquad (42)$$

is an isotropic two-body interfacial interaction. Here, $x_{12} \equiv |\mathbf{x}_1 - \mathbf{x}_2|$, while

$$\bar{\ell} = \frac{\ell(\mathbf{x}_1)+\ell(\mathbf{x}_2)}{2} \qquad (43)$$

is the arithmetic mean interfacial height. For thick wetting films, $\kappa\ell \gg 1$, we can approximate

$$U(x;\ell) \approx \frac{b_1\kappa}{2\pi\ell}\mathrm{e}^{-2\kappa\ell}\,\mathrm{e}^{-\kappa x^2/4\ell} \qquad (44)$$

which is equivalent to writing the Ω_1^2 diagram as

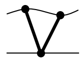 $$\approx \int\int \mathrm{d}\mathbf{s}_1\, \mathrm{d}\mathbf{s}_2 \mathrm{e}^{-\kappa\ell(\mathbf{x}_1)} S(x_{12})\mathrm{e}^{-\kappa\ell(\mathbf{x}_2)} \qquad (45)$$

where $S(x_{12})$ is another two-body interfacial interaction

$$S(x) = \frac{1}{4\pi\xi_{\mathrm{NL}}^2}\mathrm{e}^{-\kappa x^2/4\xi_{\mathrm{NL}}^2} \qquad (46)$$

with the form of a simple Gaussian. Here, we have identified the characteristic length of the Gaussian repulsion as

$$\xi_{\mathrm{NL}} = \sqrt{\frac{\ell}{\kappa}} \qquad (47)$$

which is where the new length-scale in the NL description arises. The integrated strength of S is unity.

The presence of a two-body interaction, generated by integrating out degrees of freedom from a strictly short-ranged local LGW model, is the crucial new ingredient in the NL model and will play a central role in resolving the problems of critical wetting. The Gaussian interaction (46), has both long-ranged and short-ranged properties, decaying faster than any power law but with a characteristic length that diverges as the interface unbinds. Similar two-body interactions and length-scales arise in the higher-order diagrams which generate the hard-wall repulsion [23] and restrict the interface to $\ell(\mathbf{x}) > 0$. Three-body interfacial interactions are important for tricritical wetting but will not be considered here [23].

2.4. CW and FJ models as long-wavelength approximations

The CW and FJ models can be recovered as long-wavelength approximations to the NL model which now sheds new light on their origin and validity. Consider first the Ω_1^1 diagram (40) which, for planar walls, remains a local interaction. Expanding, $\sqrt{1+(\nabla\ell)^2} = 1 + (\nabla\ell)^2/2 + \cdots$ recovers the leading-order exponential decays in the binding potential and stiffness-coefficient appearing in the FJ model and explains why their coefficients are the same. These remain valid approximations provided the gradient is small which is true at length-scales much larger than the bulk correlation length. The NL model therefore has nothing new to say about these terms in the FJ model.

This is not the case for the Ω_1^2 diagram describing the bare repulsion in the binding potential. For *fixed* $\xi_{\rm NL}$, the Fourier transform of the two-body Gaussian is

$$\mathcal{S}(q) = {\rm e}^{-q^2\xi_{\rm NL}^2} \tag{48}$$

and decays very quickly for wavenumbers $q > 1/\xi_{\rm NL}$. The CW and FJ models do not describe this correctly (see figure 3) and are equivalent to the small q approximations

$$\mathcal{S}_{\rm CW}(q) \approx 1 \tag{49}$$

and

$$\mathcal{S}_{\rm FJ}(q) \approx 1 - q^2\xi_{\rm NL}^2 \tag{50}$$

respectively. Inverting these expressions, we see that they are equivalent to setting, in real space,

$$S_{\rm CW}(x) \approx \delta(\mathbf{x}_{12}) \tag{51}$$

and

$$S_{\rm FJ}(x) \approx \left(1 - \kappa\ell(\nabla\ell)^2\right)\delta(\mathbf{x}_{12}) \tag{52}$$

which recovers, immediately, the CW and FJ models from the NL theory. These are both rather poor treatments of the two-body interaction because they fail to account properly for the second parallel length-scale $\xi_{\rm NL}$. In particular, the second term in the last expression generates the troublesome polynomial correction in the FJ stiffness-coefficient, proportional to $-\ell{\rm e}^{-2\kappa\ell}$, which leads to the stiffness-instability. This is only valid for small wavevectors and is completely inadequate for $q > 1/\xi_{\rm NL}$, where it gets the *sign* of the interaction wrong. This is the source of the stability problem in the FJ model which can now be seen as an artefact of using the long-wavelength approximation over the entire wavevector range. In reality, the two-body interaction is always repulsive and therefore no stiffness-instability is ever possible. Similarly, the CW model overestimates the strength of the repulsion from the wall for wavevectors $q > 1/\xi_{\rm NL}$. The actual repulsion is weaker at these length-scales. The above remarks highlight the essential new physics contained in the non-local model.

3. Mean-field correlations revisited: two parallel length-scales

3.1. The LGW model

Before we consider the influence of the new length-scale $\xi_{\rm NL}$ on the RG predictions, we show that its presence can be seen directly from analysis of correlation functions within a microscopic theory. To this end, we return to the starting

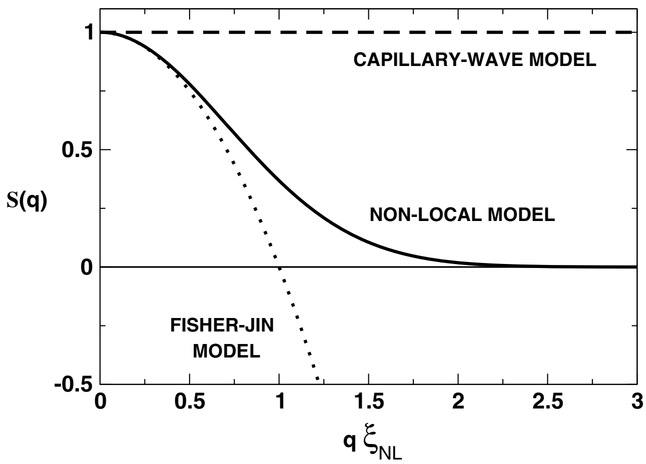

Figure 3. The Fourier transform $\mathcal{S}(q)$ of the two-body interfacial interaction $S(x)$ describing the direct interfacial repulsion from the wall for critical wetting. The FJ expression gets the sign of the interaction wrong for wavenumbers $q > 1/\xi_{\rm NL}$, which is the source of the apparent stiffness-instability in their theory. The repulsion is weaker in the NL theory than in the original CW description, leading to thinner wetting films and a smaller asymptotic critical regime.

point of wetting theory itself [37] and consider the mean-field treatment of the LGW Hamiltonian [6]

$$H_{\rm LGW}[m] = \int {\rm d}\mathbf{r}\left\{\tfrac{1}{2}(\nabla m)^2 + \phi(m)\right\} \tag{53}$$

based on a magnetization-like order-parameter $m(\mathbf{r})$. The system is bounded by a planar wall in the $z = 0$ plane and we consider the simplest choice of boundary condition with fixed surface magnetization $m = m_1 > 0$. For this model, first-order wetting transitions do not arise and the surface phase diagram is particularly simple showing only critical and complete wetting behaviour (figure 2). A bulk potential $\phi(m)$ describes the coexistence of bulk phases α and β (in zero bulk field $h = 0$) which we associate with negative and positive magnetizations, respectively. For simplicity, we impose Ising symmetry so that in zero field $m_\beta = -m_\alpha = m_0$ where $m_0 = m_0(T)$ is the spontaneous magnetization. In order to generate a wetting layer of the β phase, we suppose we are below the bulk critical temperature and $h \leqslant 0$, so that infinitely far from the wall the bulk magnetization is negative corresponding to phase α. We identify the thickness of the adsorbed wetting layer from $m(\hat{\ell}) = 0$, where $m(z) = \langle m(r)\rangle$ is the equilibrium magnetization profile.

Minimizing (53) leads to the familiar Euler–Lagrange equation for the mean-field profile

$$m''(z) = \phi'(m) \tag{54}$$

which is solved subject to $m(0) = m_1$ and $m(\infty) = m_\alpha$. This has a well known graphical solution due to Cahn [37] valid for quite general choices of the potential $\phi(m)$ and indicates the presence of a critical wetting transition at temperature $T_{\rm w}$ for which $m_1 = m_0(T)$. For temperatures such that $m_1 > m_0(T)$, the wall-α interface is completely wet by the β phase corresponding to zero contact angle. For critical wetting, it is convenient to define the temperature-like scaling field

$$\tau \equiv \frac{m_1 - m_0}{m_0} \quad (55)$$

which is also an appropriate definition beyond mean-field, in 3D, provided we restrict attention to $\omega < 2$.

We wish to calculate the pair-correlation function $G(\mathbf{r}_1, \mathbf{r}_2) = \langle m(\mathbf{r}_1)m(\mathbf{r}_2)\rangle - \langle m(\mathbf{r}_1)\rangle\langle m(\mathbf{r}_2)\rangle$ and investigate its behaviour at critical and complete wetting transitions. It is convenient to exploit the translational invariance of the profile parallel to the wall and introduce the transverse or parallel Fourier transform

$$\mathcal{G}(z_1, z_2; q) \equiv \int \mathrm{d}\mathbf{x}_{12}\, \mathrm{e}^{\mathrm{i}\mathbf{q}\cdot\mathbf{x}_{12}} G(\mathbf{r}_1, \mathbf{r}_2) \quad (56)$$

where $\mathbf{x}_{12}$ is the parallel displacement vector between the two points at heights z_1 and z_2, respectively. At mean-field level, the Ornstein–Zernike equation for G reduces to the differential equation

$$\left(-\partial_{z_1}^2 + \Phi''(m(z_1)) + q^2\right)\mathcal{G}(z_1, z_2; q) = \delta(z_1 - z_2) \quad (57)$$

and vanishes when one particle is at the wall due to the choice of fixed boundary conditions. In writing this, we have set $k_B T = 1$ for convenience.

A closed form expression for $\mathcal{G}(z_1, z_2; q)$ may be obtained within the double-parabola (DP) approximation [44, 45, 14, 22]

$$\phi(m) = \frac{\kappa^2}{2}(|m| - m_0)^2 - hm \quad (58)$$

which contains all the essential physics necessary for a description of critical and complete wetting transition. Here κ denotes the inverse bulk correlation length which, for simplicity, we assume to be independent of the bulk field. The profile $m(z)$ is readily calculated in the DP approximation and leads to a film thickness

$$\kappa\hat{\ell} = -\ln\left\{-\frac{\tau}{2} + \frac{h}{2m_0\kappa^2} + \sqrt{\frac{(\tau - h/m_0\kappa^2)^2}{4} - \frac{h}{m_0\kappa^2}}\right\}. \quad (59)$$

This recovers the well known logarithmic divergences for both critical wetting (paths (A) and (B)) and complete wetting (path C) transitions.

The calculation of the correlation function is also straightforward provided one allows correctly for the delta functions appearing in $\phi''(m)$. We only quote the result in the region of most interest where the particle positions are within the wetting layer and verify $0 \leqslant z_1 \leqslant z_2 \leqslant \hat{\ell}$. The solution separates conveniently into singular and regular parts

$$\mathcal{G}(z_1, z_2; q) = \mathcal{G}^{\mathrm{sing}}(z_1, z_2; q) + \mathcal{G}^{\mathrm{reg}}(z_1, z_2; q) \quad (60)$$

both of which have physical interpretations. Defining

$$\kappa_q \equiv \sqrt{\kappa^2 + q^2} \quad (61)$$

the regular contribution is

$$\mathcal{G}^{\mathrm{reg}}(z_1, z_2; q) = \frac{\sinh(\kappa_q z_1)\sinh(\kappa_q(\hat{\ell} - z_2))}{\kappa_q \sinh(\kappa_q \hat{\ell})} \quad (62)$$

and contains no parallel length-scales that diverge as $\ell \to \infty$. The function G^{reg} can be identified as the correlation function for a thin film with two surfaces of fixed magnetization: $m = m_1$ at $z = 0$ and $m = 0$ at $z = \hat{\ell}$. The regular contribution vanishes if a particle is at one of these planes. It carries no information arising from interfacial fluctuations which are instead described by the singular contribution

$$\mathcal{G}^{\mathrm{sing}}(z_1, z_2; q) = \frac{\Psi(z_1; q)\Psi(z_2; q)}{E(q)}. \quad (63)$$

Here

$$\Psi(z; q) = m_0\kappa \frac{\sinh \kappa_q z}{\sinh \kappa_q \hat{\ell}} \quad (64)$$

and

$$\frac{E(q)}{\kappa^2 m_0^2} = \frac{2\kappa_q}{1 - \mathrm{e}^{-2\kappa_q\hat{\ell}}} - \frac{2\kappa}{1 - h/m_0\kappa^2}. \quad (65)$$

The simple product nature of the singular contribution is reminiscent of the leading term in a spectral expansion with Ψ playing the role of the ground state eigenfunction [46]. We want to emphasize, however, that the result (63) contains the full wavevector dependence implicit in the complete spectral expansion. The simplicity of the closed form expression for $\mathcal{G}(z_1, z_2; q)$, which is available in the DP approximation, has a number of advantages over other approaches which have focused either on the moments of the correlation function or its spectral expansion [46–48].

3.2. Two diverging parallel length-scales

Next, we consider what in mean-field theory can be considered the scaling limit. We focus on thick wetting films $\kappa\hat{\ell} \gg 1$ and wavelengths long compared to the bulk correlation length, $q \ll \kappa$. The distances z_1 and z_2 are left arbitrary but we suppose they are each more than (say) one bulk correlation length from the wall. In these limits, we can approximate

$$\Psi(z; q) \approx m_0\kappa\, \mathrm{e}^{\kappa_q(z - \hat{\ell})}. \quad (66)$$

Notice that the decay length of the exponential is wavevector dependent and not precisely equal to the bulk correlation length. Similarly,

$$E(q) \approx 2m_0\kappa|h| + 2m_0^2\kappa^3\mathrm{e}^{-2\kappa\hat{\ell} - q^2\hat{\ell}/\kappa} + \sigma_{\alpha\beta}q^2 + \cdots \quad (67)$$

where $\sigma_{\alpha\beta} = m_0^2\kappa$ is the surface tension of the free $\alpha\beta$ interface for the DP potential [22]. The wavevector dependence of $E(q)$ is therefore characterized by two diverging length-scales. The larger of these is the usual parallel correlation length identified as

$$\xi_\parallel = \sqrt{\frac{\sigma_{\alpha\beta}}{E(0)}}. \quad (68)$$

This is the analogue of the length $\sqrt{\Sigma/W''(\hat{\ell})}$ appearing in the CW model. However there is also a second coherence length

$$\hat{\xi}_{\rm NL} = \sqrt{\frac{\hat{\ell}}{\kappa}} \tag{69}$$

which also diverges as the film grows. This is clearly the mean-field value of length-scale (47) describing the two-body interfacial interaction $S(x)$ which appears in the NL model. Equivalently we can write $\kappa\hat{\xi}_{\rm NL} \propto \sqrt{\ln(\kappa\xi_\parallel)}$ which implies that $\hat{\xi}_{\rm NL}$ is similar to the roughness of the $\alpha\beta$ interface induced by thermal fluctuations. The closed form expression for the pair-correlation function contains detailed information concerning both the manifestation and damping of fluctuation effects at 3D wetting brought about by the second length-scale.

Consider for example, the approach to critical wetting at bulk coexistence (path A). Within the wetting layer, the magnetization profile is simply

$$m(z) = m_0 - m_0 {\rm e}^{\kappa(z-\hat{\ell})} \tag{70}$$

where $\kappa\hat{\ell} = \ln(m_0/(m_0 - m_1))$. A similar exponential decay, controlled by the bulk correlation length, happens for $z > \hat{\ell}$. Near the $\alpha\beta$ interface, the correlation function is

$$\mathcal{G}(\hat{\ell}, \hat{\ell}; q) \approx \frac{\mathcal{G}(\hat{\ell}, \hat{\ell}; 0)}{{\rm e}^{-q^2\hat{\xi}_{\rm NL}^2} + q^2\xi_\parallel^2} \tag{71}$$

where, the zeroth moment

$$\mathcal{G}(\hat{\ell}, \hat{\ell}; 0) = \frac{m'(\hat{\ell})^2\xi_\parallel^2}{\sigma_{\alpha\beta}}. \tag{72}$$

Here $m'(\hat{\ell}) = -\kappa m_0$ is the gradient of the magnetization profile at the location of the interface. The parallel correlation length satisfies

$$\xi_\parallel^2 = \frac{\sigma_{\alpha\beta}}{2m_0^2\kappa^3\tau^2} \tag{73}$$

which identifies the mean-field critical wetting exponent $\nu_\parallel^{\rm MF} = 1$. The expression for the zeroth moment has been discussed many times before and has a simple interpretation which is correctly captured by the capillary-wave theory. In the strict $q \to 0$ limit, magnetization fluctuations arise from translations in the interfacial height and we expect $\mathcal{G}(\hat{\ell}, \hat{\ell}; 0) = m'(\ell)^2\mathfrak{g}(0)$ where $\mathfrak{g}(q)$ is the Fourier transform of the height–height correlation function. The CW expression (9) gets this bit right.

However, comparison of (71) and (9) reveals that the wavevector dependence of the LGW correlation function is more involved than in the simple CW theory due to presence of the second length-scale. Specifically the denominator of (71) is only well approximated by $1 + q^2\xi_\parallel^2$, as predicted by CW theory, provided the wavenumbers satisfy $q < 1/\hat{\xi}_{\rm NL}$ and *not* $q < \kappa$ as previously assumed. Since $\hat{\xi}_{\rm NL}$ diverges as the interface unbinds, this implies that a broad part of the interfacial spectrum has been treated incorrectly. A clue to what is happening in the regime $1/\hat{\xi}_{\rm NL} < q < \kappa$ can be read directly from the LGW result (71). In this case, the first term in the denominator can be neglected and

$$\mathcal{G}(\hat{\ell}, \hat{\ell}; q) \approx \frac{m'(\ell)^2}{q^2\sigma_{\alpha\beta}}. \tag{74}$$

This is the same as the result for the correlation function for a *free* $\alpha\beta$ interface infinitely far from a wall. In other words, for critical wetting, interfacial fluctuations with wavenumbers in the range $1/\hat{\xi}_{\rm NL} < q < \kappa$ appear to be independent of the presence of the substrate. This feature is not specific to the double-parabola approximation. For example, it can also be seen in the correlation function $\mathcal{G}(z_1, z_2; q)$ calculated for the potential $\phi(m) = -rm^2/2 + um^4/4$ (in zero bulk field). Indeed, it is implicit in the equations derived by Brezin, Halperin and Leibler [46] in their original examination of the upper critical dimension for wetting (see their equations (26a)–(26e), noting there is a missing $\mp$ sign in the argument of the exponential in (26a)). These authors concentrated on extracting the dominant length-scale $\xi_\parallel$ and did not notice the property (74).

There is more evidence for different interfacial behaviour in this wavevector range when we consider the correlation function away from the interface. Directly from (63), the singular contribution is

$$\mathcal{G}^{\rm sing}(z_1, z_2; q) \approx {\rm e}^{\kappa_q(z_1-\hat{\ell})}{\rm e}^{\kappa_q(z_2-\hat{\ell})}\mathcal{G}(\hat{\ell}, \hat{\ell}; q) \tag{75}$$

which is valid for both critical and complete wetting. Only at $q = 0$ may we associated each exponential with the derivative of the profile (70). More generally the inverse decay length is $\kappa_q = \sqrt{\kappa^2 + q^2}$. If one or both particle positions are near the wall, this introduces significant new wavevector dependence controlled by the length-scale $\hat{\xi}_{\rm NL}$. For example, the correlation function near the wall is

$$\mathcal{G}^{\rm sing}(0, 0; q) \approx {\rm e}^{-2\kappa\hat{\ell}}\mathcal{G}(\hat{\ell}, \hat{\ell}; q){\rm e}^{-q^2\hat{\xi}_{\rm NL}^2} \tag{76}$$

which for critical wetting (path A) reduces to

$$\mathcal{G}^{\rm sing}(0, 0; q) \approx \frac{1}{2\kappa}\frac{{\rm e}^{-q^2\hat{\xi}_{\rm NL}^2}}{{\rm e}^{-q^2\hat{\xi}_{\rm NL}^2} + q^2\xi_\parallel^2}. \tag{77}$$

The zeroth moment $G_0^{\rm sing}(0, 0) \equiv \mathcal{G}^{\rm sing}(0, 0; 0) = \frac{1}{2\kappa}$ remains finite at the phase transition. This is consistent with an exact sum-rule $G_0^{\rm sing}(0, 0) \approx (-t)^{-\alpha_s}$ where $\alpha_s^{\rm MF} = 0$ is the mean-field value of the specific heat exponent [36]. A more telling feature is that the presence of the exponential damping in the numerator implying that the singular contribution is *strongly suppressed* for wavenumbers $q > 1/\hat{\xi}_{\rm NL}$. Essentially, there is no singular contribution to $\mathcal{G}(0, 0; q)$ in this range of wavevectors. Interfacial fluctuations are damped long before we reach the scale of the bulk correlation length ξ_β. There are a number of consequences of this damping to which we will return later.

Finally, we note that the presence of two diverging parallel length-scales in the structure factor $\mathcal{G}(z_1, z_2; q)$ has implications for the *true* correlation length $\xi_\parallel^{\rm T}$ characterizing

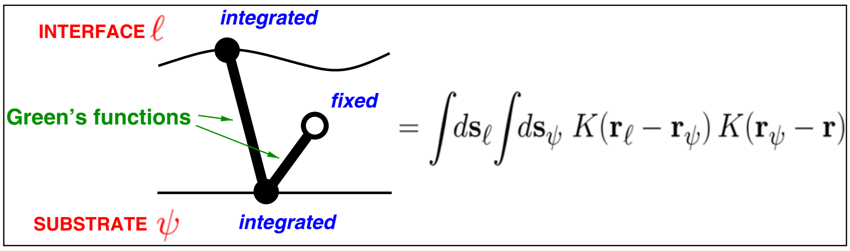

Figure 4. Example of a wetting diagram and its algebraic expression.

the asymptotic large distance, $x_{12} \to \infty$, decay of the pair-correlation function $G(\mathbf{r}_1, \mathbf{r}_2) \approx \mathrm{e}^{-x_{12}/\xi_\parallel^{\mathrm{T}}}$. This is determined, in standard fashion, through the zero of the function $E(q)$ lying on the imaginary axis of q, considered in the complex plane:

$$E\left(\mathrm{i}/\xi_\parallel^{\mathrm{T}}\right) = 0. \tag{78}$$

Thus, along path A, the true correlation length is found from the solution of

$$\mathrm{e}^{\hat{\xi}_{\mathrm{NL}}^2/(\xi_\parallel^{\mathrm{T}})^2} = \frac{\xi_\parallel^2}{(\xi_\parallel^{\mathrm{T}})^2} \tag{79}$$

hence

$$(\xi_\parallel^{\mathrm{T}})^2 \approx \xi_\parallel^2 - \hat{\xi}_{\mathrm{NL}}^2. \tag{80}$$

The true correlation length is therefore slightly smaller than $\xi_\parallel$ and contains a singular correction term. Within the CW theory no such distinction between the length-scales $\xi_\parallel$ and $\xi_\parallel^{\mathrm{T}}$ arises.

3.3. Correlation functions within the NL model

In this section, we show that the NL theory reproduces the LGW result for the singular contribution to the pair-correlation function and has a simple diagrammatic formulation. To show this we will need to reproduce some details of the derivation of the NL model [22, 23]. The starting point for the derivation is the LGW model (53) generalized to allow for non-planar walls described by a height function $\psi(\mathbf{x})$ but with the same choice of fixed magnetization boundary conditions $m(\mathbf{r}_\psi) = m_1$ where $\mathbf{r}_\psi = (\mathbf{x}, \psi)$ is an arbitrary point on the wall. The wall is in contact with the bulk phase α and preferentially adsorbs a film of the β phase. A collective coordinate $\ell(\mathbf{x})$ denotes the location of a surface of iso-magnetization $m(\mathbf{r}_\ell) = 0$ where $\mathbf{r}_\ell = (\mathbf{x}, \ell)$ is an arbitrary point on the $\alpha\beta$ interface. This is the cross-criterion definition of the interfacial height. The interfacial Hamiltonian is then defined following the recipe of Fisher and Jin [14]

$$H[\ell, \psi] = H[m_\Xi] - F_{\mathrm{w}\beta}[\psi] \tag{81}$$

where $F_{\mathrm{w}\beta}[\psi]$ is the excess free-energy of the wall-β interface. Here, $m_\Xi(\mathbf{r})$ is the magnetization that minimizes the LGW Hamiltonian subject to the crossing criterion constraint $m(\mathbf{r}_\ell) = 0$ and wall and bulk boundary conditions. Within the DP approximation, this solves the Helmholtz equation

$$\nabla^2 m = \kappa^2 (m - m_0) \tag{82}$$

where we have assumed, for simplicity, $h = 0$ and have focused only on the magnetization within the wetting layer ($m > 0$). This is solved using a multiple reflection expansion involving surface integrals of the Green's function $K(\mathbf{r}_1, \mathbf{r}_2)$ given in (36). We represent K diagrammatically by a straight thick line with the open circles denoting the end points

$$K(\mathbf{r}_1, \mathbf{r}_2) = \quad . \tag{83}$$

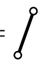

Using this, we can write the constrained magnetization

$$m_\Xi(\mathbf{r}) = m_0 - m_0 \left(\quad - \quad + \quad - \cdots \right) + \delta m_1 \left(\quad - \quad + \quad - \cdots \right) \tag{84}$$

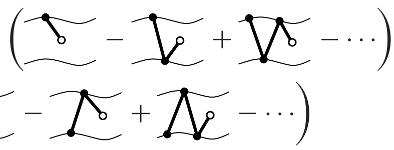

where $\delta m_1 = m_1 - m_0$ and the interpretation of the wavy-lines, representing the interface and wall, and also the black dot (surface integral) is as before. This is illustrated in figure 4. The expression (84) is an exact solution to the Helmholtz equation, and satisfies the boundary conditions at the interface and wall to exponentially accurate order in the radii of curvature. On substitution into (81) and after some algebra, we arrive at the non-local model (32) with geometry independent coefficients

$$\frac{a}{\sigma_{\alpha\beta}} = 2\tau, \qquad \frac{b_1}{\sigma_{\alpha\beta}} = 1, \qquad \frac{b_2}{\sigma_{\alpha\beta}} = \tau^2. \tag{85}$$

The derivation of the model can be readily extended to non-zero bulk fields $h < 0$ [49]. This generates the thermodynamic contribution $\bar{V}_\beta$ (see (32)) where $\bar{h} = 2m_0|h|$ and has only very minor influence on the coefficients $a, b_1, b_2, \ldots$ which can be safely ignored.

The NL model provides a simple explanation of correlation function structure at 3D wetting. Key to this is the relationship between fluctuations (correlations) in the interfacial height $\ell(\mathbf{x})$ and fluctuations (correlations) in the microscopic order-parameter $m(\mathbf{r})$. Consider again the connected height–height correlation function

$$g(\mathbf{x}_1, \mathbf{x}_2) \equiv \langle \delta\ell(\mathbf{x}_1)\delta\ell(\mathbf{x}_2)\rangle. \tag{86}$$

At mean-field level, this follows simply from solution of the interfacial version of the Ornstein–Zernike equation

$$\int \mathrm{d}\mathbf{x}_3\, c(\mathbf{x}_1, \mathbf{x}_3) g(\mathbf{x}_3, \mathbf{x}_2) = \delta(\mathbf{x}_1 - \mathbf{x}_2). \tag{87}$$

Here, the direct interfacial correlation function is defined in the usual way as the second-functional derivative of the interfacial

Hamiltonian (setting $k_B T = 1$):

$$c(\mathbf{x}_1, \mathbf{x}_2) = \frac{\delta^2 H[\ell]}{\delta\ell(\mathbf{x}_1)\delta\ell(\mathbf{x}_2)} \tag{88}$$

where the derivatives are evaluated at the equilibrium interfacial profile $\hat{\ell}$. For the case of wetting at planar substrates, both $c(\mathbf{x}_1, \mathbf{x}_2)$ and $g(\mathbf{x}_1, \mathbf{x}_2)$ depend only on the transverse separation $x_{12} = |\mathbf{x}_1 - \mathbf{x}_2|$. Consequently, their Fourier transforms, defined analogous to (8), satisfy

$$\mathfrak{g}(q) = \frac{1}{\tilde{c}(q)}. \tag{89}$$

For the non-local model (38), the functional derivatives required to generate c are readily performed. Using only the dominant diagrams Ω_1^1 and Ω_1^2, we find

$$\tilde{c}(q) = 2\kappa m_0|h| + 2b_1\kappa^2 e^{-2\kappa\hat{\ell}} \mathcal{S}(q) + \sigma_{\alpha\beta} q^2 + \cdots. \tag{90}$$

Here $\mathcal{S}(q) = e^{-q^2\xi_{\rm NL}^2}$ is the Fourier transform of the two-body interfacial interaction discussed earlier. This reproduces the long-wavelength expression for $E(q)$ appearing in the LGW calculation.

The explicit relationship between the constrained magnetization and the interfacial configuration identifies the corresponding connected magnetization–magnetization correlation function as

$$\langle \delta m(\mathbf{r}_1)\delta m(\mathbf{r}_2)\rangle = \int\int \mathrm{d}\mathbf{x}_3\, \mathrm{d}\mathbf{x}_4 \frac{\delta m_\Xi(\mathbf{r}_1)}{\delta\ell(\mathbf{x}_3)} \frac{\delta m_\Xi(\mathbf{r}_2)}{\delta\ell(\mathbf{x}_4)} g(\mathbf{x}_3, \mathbf{x}_4). \tag{91}$$

The functional derivative of m_Ξ is easily determined from the expansion (84). Only the first term, containing a single kernel, is of importance (the reflections giving rise to exponentially small corrections). The leading contribution to the magnetization correlation function, within the NL theory, is therefore

$$\frac{G_{\rm NL}(\mathbf{r}_1, \mathbf{r}_2)}{m_0^2} = \frac{\partial^2}{\partial z_1\, \partial z_2} \times \int\int \mathrm{d}\mathbf{x}_3\, \mathrm{d}\mathbf{x}_4\, K(\mathbf{r}_1, \mathbf{r}_3) g(\mathbf{x}_3, \mathbf{x}_4) K(\mathbf{r}_4, \mathbf{r}_2) \tag{92}$$

where $\mathbf{r}_i = (\mathbf{x}_i, \hat{\ell})$ is a point on the interface ($i = 3, 4$). This has the short-hand diagrammatic representation

$$\frac{G_{\rm NL}(\mathbf{r}_1, \mathbf{r}_2)}{m_0^2} = \frac{\partial^2}{\partial z_1 \partial z_2} \tag{93}$$

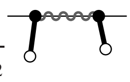

where the wiggly line represents the height–height correlation function $g(x_{12})$.

To continue, we take the Fourier transform of (92) and arrive at our final result

$$G_{\rm NL}(z_1, z_2; q) = m_0^2 \frac{\tilde{K}'(z_1 - \hat{\ell}; q)\tilde{K}'(z_2 - \hat{\ell}; q)}{\tilde{c}(q)} \tag{94}$$

where

$$\tilde{K}(z; q) = \frac{\kappa}{\kappa_q} e^{-\kappa_q|z|} \tag{95}$$

is the transverse Fourier transform of the Green's function (36) and the prime denotes the derivative w.r.t. z. It is clear that $\Psi(z, q) \approx m_0 \tilde{K}'(z - \hat{\ell}; q)$, implying $G_{\rm NL} \approx G_{\rm sing}$. Thus, the NL theory describes correctly the position dependence of the singular contribution to the magnetization correlation function. One may picture the singular or interfacial contribution to the magnetization correlation function arising in the following manner: bulk-like correlations represented by the Ornstein–Zernike-like function (36) connect each of the two points $\mathbf{r}_1$ and $\mathbf{r}_2$ to different points on interface which are themselves correlated by the interfacial fluctuations. Again, it is tempting to associate each bulk-like correlation as itself arising from tube-like fluctuations but this is not needed explicitly. However, the scaling relation between the second parallel correlation length and the interfacial height, $\xi_{\rm NL} \sim \ell^{1/2}$, is strikingly similar to the transverse wandering induced by the thermal fluctuations of a one-dimensional object of length ℓ.

3.4. *Correlation functions at complete wetting and Henderson's sum-rule*

Our paper is primarily concerned with the problems of critical wetting theory. It turns out, however, that the NL description also helps explain a problem that has been discussed in the context of the complete wetting transition. This is related to the interpretation of exact statistical mechanical sum-rules [36].

Consider correlation functions in the approach to complete wetting (path C in the surface phase diagram). The second term in (67), which depends on the length-scale $\xi_{\rm NL}$, is now of negligible importance. Consequently, the mean-field correlation function near the $\alpha\beta$ interface is

$$\mathcal{G}(\hat{\ell}, \hat{\ell}; q) \approx \frac{m_0\kappa^2}{2m_0\kappa|h| + \sigma_{\alpha\beta}q^2} \tag{96}$$

which identifies the parallel correlation length

$$\xi_\parallel = \sqrt{\frac{\sigma_{\alpha\beta}}{2m_0\kappa|h|}}. \tag{97}$$

This reproduces the well known result for the correlation function critical exponent at complete wetting $\nu_\parallel^{\rm co} = 1/2$ [1]. The wavevector dependence is simpler than the analogous result for critical wetting (71) and has a Ornstein–Zernike-like form that is captured correctly by the CW theory. This is because the dominant interfacial repulsion in the binding potential is now described by the local term Ω_1^1, rather than the non-local term Ω_1^2. Thus, the second parallel length-scale $\xi_{\rm NL}$ does not have any significant importance for correlation function structure near the unbinding interface.

However, the wavevector dependence becomes more involved as we move away from the interface. The singular contribution to G is given by

$$\mathcal{G}^{\rm sing}(z_1, z_2; q) \approx \frac{\Psi(z_1; q)\Psi(z_2; q)}{2m_0\kappa|h| + \sigma_{\alpha\beta}q^2} \tag{98}$$

where the position dependence arises from $\Psi(z; q) \approx m_0\kappa e^{\kappa_q(z-\hat{\ell})}$. Thus, when both particles are near the wall

$$\mathcal{G}^{\rm sing}(0, 0; q) \propto \frac{h^2}{2m_0\kappa|h| + \sigma_{\alpha\beta}q^2} e^{-\hat{\ell}q^2/\kappa} \tag{99}$$

where the coefficient of proportionality is $\propto(T - T_{\rm w})^{-2}$ and remains finite since $T > T_{\rm w}$. The final term is the damping factor $e^{-q^2\hat{\xi}_{\rm NL}^2}$, discussed earlier, which we have written explicitly in terms of the film thickness.

Defining the moment expansion

$$\mathcal{G}(z_1, z_2; q) = G_0(z_1, z_2) - q^2 G_2(z_1, z_2) + \cdots \qquad (100)$$

we are led to the identifications $G_0^{\rm sing}(0,0) \propto h$ and, more interestingly,

$$G_2^{\rm sing}(0,0) \propto \sigma_{\alpha\beta} + 2m_0|h|\hat{\ell}. \qquad (101)$$

This may be compared with a exact many-body theory sum-rule due to Henderson [34] for complete drying by vapour (phase β) at the interface between a purely hard-wall and a bulk liquid (α):

$$G_2(0,0) = \sigma_{\rm w\alpha} \qquad (102)$$

where $\sigma_{\rm w\alpha}$ is the total surface tension of the wall-α interface written in units of $k_{\rm B}T$. It is natural to identify the singular contribution to the second moment, $G_2^{\rm sing}(0,0) = G_2(0,0) - G_2^{\rm reg}(0,0)$, where we have simply subtracted the regular contribution $G_2^{\rm reg}(0,0) = \sigma_{\rm w\beta}$ corresponding to the correlation function for the wall-β interface. Therefore, Henderson's exact sum-rule for the singular contribution is

$$G_2^{\rm sing}(0,0) = \sigma_{\alpha\beta} + \sigma_{\rm sing} \qquad (103)$$

where $\sigma_{\rm sing}$ is the singular contribution to the excess-free-energy. In mean-field approximation, $\sigma_{\rm sing} = W(\hat{\ell})$, which for short-ranged forces is simply $\sigma_{\rm sing} \approx 2m_0|h|\hat{\ell}$, yielding $\sigma_{\rm sing} \sim \bar{h}\ln\bar{h}$.

Therefore, there are two singular contributions to the second moment $G_2(0,0)$; a finite, leading term equated with the interfacial tension $\sigma_{\alpha\beta}$ and a next-to-leading non-analytic contribution $\sigma_{\rm sing}$. Importantly, (101) includes both these terms needed to fully satisfy the exact sum-rule (103). Previously it has not been clear how the contribution $\sigma_{\rm sing}$ to $G_2(0,0)$ could arise within the framework of an effective Hamiltonian description. Within the NL theory, its origin can be traced explicitly to the expansion of the damping term $e^{-q^2\hat{\xi}_{\rm NL}^2}$ in (99) and, hence, to the role played by the second diverging length-scale. If this term were not present, the sum-rule would not be satisfied. Since the sum-rule is exact, it provides insight into what is happening beyond mean-field. Recall that, for three-dimensional systems with short-ranged forces, the mean-field predictions for complete wetting are not significantly altered by fluctuation effects. This was considered explicitly by Fisher and Huse [3] using the linear RG analysis of the CW model. The parallel correlation length retains its mean-field expression $\xi_\parallel = (\sigma_{\alpha\beta}/(2m_0\kappa|h|))^{1/2}$, while the equilibrium wetting layer thickness grows logarithmically as coexistence is approached, similar to the mean-field prediction but with a modified critical amplitude. Thus, provided $\omega < 2$, one finds $\kappa\langle\ell\rangle \approx (2+\omega)\ln\xi_\parallel$ with a similar result for $\omega > 2$. Also, the singular contribution to the free-energy $\sigma_{\rm sing} \approx 2m_0|h|\langle\ell\rangle$, similar to the mean-field critical behaviour. The up-shot of these considerations is that the expressions (99) and (101) remain valid beyond mean-field and satisfy Henderson's exact sum-rule, provided we simply replace the mean-field film thickness with the equilibrium value $\langle\ell\rangle$. This is strongly suggestive that, for all values of ω, the correlation function structure is determined by two diverging parallel length-scales $\xi_\parallel$ and $\xi_{\rm NL} = \sqrt{\langle\ell\rangle\xi_\beta}$.

4. The Ginzburg criterion revisited: reduction of the critical regime

Let us consider the path to critical wetting at bulk coexistence (path A) as described by an interfacial Hamiltonian $H[\ell]$ (CW or NL). Following standard methods, we expand the Hamiltonian to quadratic order about the mean-field interfacial location $\hat{\ell}$ and perform the Gaussian functional integrals. This generates the usual (one-loop) correction to the appropriate free-energy which in our case is the singular contribution to the surface tension of the wall-α interface. In three dimensions, this reads

$$\sigma_{\rm sing}^{(1)} = \sigma_{\rm sing}^{(0)} - \frac{k_{\rm B}T}{4\pi}\int_0^\Lambda {\rm d}q\, q\ln\tilde{c}(q). \qquad (104)$$

The zeroth-order mean-field result $\sigma_{\rm sing}^{(0)} \propto -\tau^2$ is the same in both the CW and NL theories. Differences emerge in the expression for the interfacial direct correlation function. For the CW model,

$$\tilde{c}_{\rm CW}(q) = \Sigma q^2 + \Sigma\xi_\parallel^{-2} \qquad (105)$$

in contrast with

$$\tilde{c}_{\rm NL}(q) = \Sigma q^2 + \Sigma\xi_\parallel^{-2}\mathcal{S}(q) \qquad (106)$$

for the NL theory. Here, $\xi_\parallel \sim (-\tau)^{-1}$ is the mean-field result for the parallel correlation length and $\mathcal{S}(q) = e^{-q^2\hat{\xi}_{\rm NL}^2}$. As expected, the NL model recovers the CW model (or more correctly the FJ model) for small q, but there are significant differences when the wavenumber $q > 1/\hat{\xi}_{\rm NL}$. Derivatives of the free-energy determine thermodynamic observables and it is easiest to study the derivative of $\sigma^{\rm sing}$ w.r.t. τ which generates the singular contribution to the magnetization near the wall $m_1^{\rm sing} \sim (-\tau)^{1-\alpha_s}$. The zeroth-order mean-field result remains valid provided the one-loop correction is negligible in comparison. The interpretation here is quite straightforward since the critical wetting temperature $T_{\rm w}$ is not altered by fluctuation effects for $\omega < 2$. The derivatives are easily performed, leading to the following Ginzburg criteria. For the CW model, mean-field is valid provided

$$\frac{\kappa^2}{2\pi\Sigma}\int_0^\Lambda {\rm d}q\frac{q}{q^2+\xi_\parallel^{-2}} \ll 1 \qquad (107)$$

which reduces to

$$\ln\left(1+\Lambda^2\xi_\parallel^2\right) \ll \frac{1}{\omega}. \qquad (108)$$

This is very similar to the Ginzburg criterion derived by Halpin-Healy and Brezin [50] for the approach to critical wetting along the critical isotherm, $T = T_w$, $h \to 0^-$ (path B). The above condition ties in neatly with the RG analysis for the CW model described earlier. Comparison with the integrated flow equation (16) shows that (108) is equivalent to requiring that, at the matching point, the width of the Gaussian convolution, which essentially measures the roughness $\xi_\perp$ of the $\alpha\beta$ interface, is much smaller the bulk correlation length ξ_β.

For the NL model on the other hand, mean-field theory is valid provided

$$\frac{\kappa^2}{2\pi\Sigma}\int_0^\Lambda \mathrm{d}q\,\frac{q\mathrm{e}^{-q^2\hat{\xi}_{\mathrm{NL}}^2}}{q^2+\xi_\parallel^{-2}\mathrm{e}^{-q^2\hat{\xi}_{\mathrm{NL}}^2}} \ll 1 \tag{109}$$

which shows the dampening effect arising from the second length-scale. Remarkably, this integral converges even if the high momentum cut-off Λ is set to infinity—something which can not be done in the CW theory. It is clear that the damping factor effectively reduces the upper-limit of the integral so that we can approximate

$$\frac{\kappa^2}{2\pi\Sigma}\int_0^{\Lambda_{\mathrm{NL}}} \mathrm{d}q\,\frac{q}{q^2+\xi_\parallel^{-2}} \ll 1 \tag{110}$$

where, at this one-loop level, we can identify an effective cut-off

$$\Lambda_{\mathrm{NL}} \approx \frac{1}{\hat{\xi}_{\mathrm{NL}}}. \tag{111}$$

This expresses the fact that wavenumbers $q > 1/\hat{\xi}_{\mathrm{NL}}$ do not contribute to the one-loop correction to the surface magnetization. This is similar to the behaviour seen earlier in the mean-field correlation function $\mathcal{G}(\hat{\ell},\hat{\ell};q)$ which, recall, is independent of the presence of the wall for $q > 1/\hat{\xi}_{\mathrm{NL}}$. Thus, the Ginzburg criterion reduces to

$$\ln\left(1+\Lambda_{\mathrm{NL}}^2\xi_\parallel^2\right) \ll \frac{1}{\omega} \tag{112}$$

showing that non-locality reduces the size of the asymptotic regime. Later we shall see how this ties in with the linear RG analysis of the NL model.

The amended Ginzburg criterion also emerges very simply from the mean-field results for the correlation function obtained for the LGW model. Taking the inverse Fourier transform, the integral over all wavevectors

$$\int \mathrm{d}\mathbf{q}\,\mathcal{G}^{\mathrm{sing}}(0,0;q) = \langle\delta m_1^2\rangle \tag{113}$$

determines the singular contribution to the mean-square surface magnetization. This may be compared to the square of the mean value $\langle\delta m_1\rangle^2 = m_0^2\mathrm{e}^{-2\kappa\hat{\ell}}$ from the tail of the mean-field magnetization profile due to the $\alpha\beta$ interface. A Ginzburg criterion may, hence, be formulated as the condition

$$\int \mathrm{d}\mathbf{q}\,\mathcal{G}^{\mathrm{sing}}(0,0;q) \ll \langle\delta m_1\rangle^2 \tag{114}$$

which, on using (77), reproduces (112). Therefore, we can be confident that the Ginzburg criteria calculated using the NL interfacial Hamiltonian is the same as that pertinent to the underlying LGW theory.

Comparison of equations (108) and (112) shows that one may re-express the Ginzburg criterion for the NL model as

$$\ln(1+\Lambda^2\xi_\parallel^2) \ll \frac{1}{\omega_{\mathrm{eff}}} \tag{115}$$

where we have introduced an effective value of the wetting parameter

$$\omega_{\mathrm{eff}} = \omega\frac{\ln(1+\Lambda_{\mathrm{NL}}^2\xi_\parallel^2)}{\ln(1+\Lambda^2\xi_\parallel^2)}. \tag{116}$$

This is just as another way of expressing the reduction in the cut-off due to the dampening influence of the length-scale ξ_{NL}. For thick films, this reduces to

$$\omega_{\mathrm{eff}} = \omega - \omega\frac{\ln(\Lambda\hat{\xi}_{\mathrm{NL}})}{\ln(\Lambda\xi_\parallel)} + \cdots. \tag{117}$$

A similar expression for an effective wetting parameter also emerges from an RG analysis, which we turn to next.

5. Functional renormalization for a two-body interfacial potential

5.1. Linearized functional recursion relations

It is straightforward to generalize the linear RG analysis to account for the two-body nature of the repulsive interfacial interaction $U(x;\bar{\ell})$. Although it would have been preferable to generalize the nonlinear RG scheme [41] to assess the role played by the hard-wall condition, we have not been able to do this and, in fact, questions remain on how to model best the hard-wall using the linear RG when a non-local repulsion is present. Fortunately, these subtleties do not impact on fluctuation effects in regime (I), for which $0 < \omega < 1/2$, where the hard-wall is unimportant and the linear RG is most reliable. If a stiffness-instability does not occur in this regime, then it is certainly not present in regimes (II) and (III).

The starting point for our analysis is the small-gradient approximation,

$$H_{\mathrm{NL}}[\ell] = \int \mathrm{d}\mathbf{x}\left\{\frac{\Sigma}{2}(\nabla\ell)^2 + V(\ell)\right\} + \Delta W_{\mathrm{NL}}[\ell] \tag{118}$$

where we have split the NL binding potential functional into local and non-local contributions. The local contribution models the attractive part of the potential, and is the same as in the CW theory

$$V(\ell) = \bar{h}\ell + a\mathrm{e}^{-\kappa\ell} \tag{119}$$

where the exponential decay arises from the Ω_1^1 diagram. For the non-local interaction, we write

$$\Delta W_{\mathrm{NL}}[\ell] = \int\!\!\int \mathrm{d}\mathbf{x}_1\,\mathrm{d}\mathbf{x}_2 U(x_{12};\bar{\ell}) \tag{120}$$

where, as before,

$$U(x;\ell) = \frac{b_1\kappa^2}{2\pi}\int_{2\kappa\ell}^\infty \mathrm{d}\tau\,\frac{\mathrm{e}^{-\sqrt{\tau^2+\kappa^2x^2}}}{\sqrt{\tau^2+\kappa^2x^2}} \tag{121}$$

depends only on the arithmetic mean interfacial height $\bar{\ell}$ of the two points, and $x_{12} = |\mathbf{x}_2 - \mathbf{x}_1|$. The two-body interaction $U(x; \bar{\ell})$ accounts for the length-scale $\xi_{\rm NL}$ and is responsible for the term proportional to $-\ell e^{-2\kappa\ell}$ in the FJ stiffness, which induced the instability. The high momentum cut-off for all terms in the Hamiltonian is $\Lambda \approx \kappa$ and a hard-wall condition restricts $\ell(\mathbf{x}) > 0$. In writing this Hamiltonian, we have simplified the full NL description using the usual gradient expansion for the interfacial area $d\mathbf{s}_\ell = d\mathbf{x}\sqrt{1+(\nabla\ell)^2} \approx d\mathbf{x}(1+(\nabla\ell)^2/2)$ and discarding the position-dependent stiffness contributions which emerge trivially from this expansion. These aren't responsible for the stiffness-instability in the FJ model. However, the linear RG approach presented in this section can be easily extended to take into account these extra terms. The solution of the RG flow is technically more complicated, but the obtained results do not alter the conclusions outlined in this section [51].

Because of the linear nature of the present RG scheme, we can anticipate that the local contribution satisfies the flow equation of Fisher and Huse

$$\frac{\partial V_t}{\partial t} = 2V_t + \omega\xi_\beta^2 \frac{\partial^2 V_t}{\partial \ell^2} \tag{122}$$

implying

$$V_t(\ell) = \frac{\kappa e^{2t}}{\sqrt{4\pi\omega t}} \int_{-\infty}^{\infty} d l' V_0(\ell') e^{-\kappa^2(\ell-\ell')^2/4\omega t}. \tag{123}$$

We shall be able to establish this explicitly from the generalized flow equation for the two-body interaction if one regards V as a local (delta function) contribution to U. Following the method outlined in section 2, we split the Hamiltonian into a free part H_0,

$$H_0 = \frac{\Sigma}{2}\int d\mathbf{x}\,(\nabla\ell)^2 = \frac{\Sigma}{8\pi^2}\int^\Lambda d\mathbf{q}\, q^2|\tilde{\ell}(\mathbf{q})|^2 \tag{124}$$

where $\tilde{\ell}(\mathbf{q})$ is the Fourier transform of $\ell(\mathbf{x})$, and a perturbative part $H_1 = H_{\rm NL} - H_0$ which contains both the local and non-local contributions of the binding potential functional. The fluctuating interfacial height field is divided into $\ell(\mathbf{x}) = \ell_<(\mathbf{x}) + \ell_>(\mathbf{x})$, where $\ell_<(\mathbf{x})$ accounts for large-scale fluctuations with wavenumbers $0 < q < \Lambda/b$, and b being the rescaling factor of the RG. The fast modes $\ell_>(\mathbf{x})$ account for the large-wavenumber fluctuations ($\Lambda/b < q < \Lambda$) which are integrated out in each RG step. With this choice, the free part separates into two parts $H_0[\ell] = H_0[\ell_<] + H_0[\ell_>]$, so the Hamiltonian can be written as

$$H_{\rm NL}[\ell] = H_0[\ell_<] + H_0[\ell_>] + H_1[\ell_< + \ell_>]. \tag{125}$$

The renormalized Hamiltonian is obtained by integrating out the small-scale fluctuations $\ell_>$ in the Boltzmann factor associated with the interfacial Hamiltonian:

$$e^{-\bar{H}'_{\rm NL}[\ell_<]} \propto e^{-H_0[\ell_<]}\langle e^{-H_1[\ell_<+\ell_>]}\rangle_> \tag{126}$$

where $\langle\cdots\rangle_>$ represents an average over small-scale fluctuations $\ell_>$ weighted by a Boltzmann factor $\exp(-H_0[\ell_>])$. Assuming that the perturbative part H_1 is small in some sense, we may approximate:

$$\langle \exp(-H_1[\ell_< + \ell_>])\rangle_> \approx \exp(-\langle H_1[\ell_< + \ell_>]\rangle_>) \tag{127}$$

which corresponds to keep only the first term in the cumulant expansion of the left-hand side of (127). In this linear approach, the new Hamiltonian has the form:

$$\bar{H}'_{\rm NL}[\ell_<] = H_0[\ell_<] + \langle H_1[\ell_< + \ell_>]\rangle_> \tag{128}$$

showing that the local and non-local terms of the interfacial Hamiltonian renormalize independently. The last term of (128) corresponds to the renormalized perturbative part of the potential. The final step of the renormalization group is to rescale the coordinate $\mathbf{x}$ and the large-scale fluctuating contribution to the interfacial height field $\ell_<$ according to:

$$\begin{aligned} \mathbf{x} &\to \mathbf{x}' = \mathbf{x}/b \\ \ell_<(\mathbf{x}) &\to \ell'(\mathbf{x}') = \ell_<(\mathbf{x} = \mathbf{x}'b)/b^\zeta \end{aligned} \tag{129}$$

where the roughness exponent $\zeta = (3-d)/2$ is zero for the present three-dimensional case. Regarding the non-local part of the Hamiltonian, the special form of U, which depends on $\ell(\mathbf{x}_1)$ and $\ell(\mathbf{x}_2)$ via their mean value, makes it possible to obtain a recursion relationship for the two-body interaction. The new non-local interaction can be written as

$$\Delta W'_{\rm NL}[\ell_<] = \int\int d\mathbf{x}_1\, d\mathbf{x}_2 \left\langle U(x_{12}; \bar{\ell}_< + \bar{\ell}_>)\right\rangle_>. \tag{130}$$

As with the local contribution, this expression defines a new two-body interaction $\bar{U}'(x, \bar{\ell}_<)$ which can be obtained from U as:

$$\bar{U}'(x, \bar{\ell}_<) = \left\langle \exp\left(\bar{\ell}_> \frac{\partial}{\partial \bar{\ell}_<}\right)\right\rangle_> U(x, \bar{\ell}_<) \tag{131}$$

where $\bar{\ell}_< = (\ell_<(\mathbf{x}_1) + \ell_<(\mathbf{x}_2))/2$ and $\bar{\ell}_> = (\ell_>(\mathbf{x}_1) + \ell_>(\mathbf{x}_2))/2$. Owing to the Gaussian character of the weight factor $\exp(-H_0(\ell_>))$, the average over the short-scale fluctuations can be easily calculated as

$$\bar{U}'(x, \bar{\ell}_<) = \exp\left[\frac{\omega\xi_\beta^2}{2}\left(t + \int_{1/b}^1 du\, J_0(u\Lambda x)\right)\frac{\partial^2}{\partial\bar{\ell}_<}\right] U(x, \bar{\ell}_<) \tag{132}$$

where J_0 is a Bessel function of first kind. In the final step, we perform the coordinate and $\ell_<$ rescaling (129), so the renormalized two-body interaction $U'(x', \ell')$ is:

$$U'(x', \bar{\ell}') = b^4 \bar{U}'(x = x'b, \bar{\ell}' = \bar{\ell}). \tag{133}$$

Note that the renormalized two-body interaction remains a function of the arithmetic mean interfacial heights.

If we take $b = e^{\delta t}$ and consider the limit $\delta t \to 0$, we obtain the flow equation for the renormalized two-body interaction $U_t(x, \ell)$ up to the scale e^t as:

$$\frac{\partial U_t}{\partial t} = 4U_t + x\frac{\partial U_t}{\partial x} + \omega\xi_\beta^2\left(\frac{1+J_0(\Lambda x)}{2}\right)\frac{\partial^2 U_t}{\partial \bar{\ell}^2}. \tag{134}$$

This flow equation is solved by:

$$U_t(x, \ell) = \frac{\kappa e^{4t}}{\sqrt{4\pi\omega\Phi(x,t)}}\int d\ell'\, U_0(xe^t; \ell') e^{-\kappa^2(\ell-\ell')^2/4\omega\Phi(x,t)} \tag{135}$$

where

$$\Phi(x,t) = \int_{\Lambda x}^{\Lambda x e^t} dz \frac{1 + J_0(z)}{2z} \quad (136)$$

controls the width of the Gaussian convolution. As remarked earlier, the renormalized local potential $V_t(\ell)$ given by (123) also emerges from (136) if one regards V as a local (delta function) contribution to U.

The two remaining ingredients in the RG analysis are the matching condition and approximate handling of the hard-wall constraint. We use the simplest choice of matching procedure and integrate over the two-body interaction in order to construct a NL binding potential *function*

$$W_t^{\rm NL}(\ell) = V_t(\ell) + \Delta W_t^{\rm NL}(\ell) \quad (137)$$

where

$$\Delta W_t^{\rm NL}(\ell) \equiv \int d\mathbf{x}\, U_t(x;\ell). \quad (138)$$

The flow is then stopped when the curvature verifies $W_t''(\ell^*) = \Sigma\Lambda^2$, at ℓ^* (the minimum of $W_t(\ell)$). A more refined version of this would be to calculate the renormalized direct correlation function, defined as the second-functional derivative of the renormalized Hamiltonian, analogous to (88). The renormalized *true* correlation length could then be determined by locating the zero of its Fourier transform in the complex plane. The RG flow is then stopped when this is of order Λ^{-1}. This procedure distinguishes between the true correlation length and a length defined via the curvature of the potential (137) but does not influence the final predictions concerning the order of the phase transition.

There is some freedom of choice into how one incorporates the hard-wall, or rather, soft-wall restriction into the linear RG scheme. The most natural is to write

$$V_0(\ell) = V(\ell)\Theta(\ell) \quad (139)$$

and

$$U_0(x;\ell) = U(x;\ell)\Theta(\ell) + \frac{c}{b_1} U(x;0)\Theta(-\ell) \quad (140)$$

for the bare local and non-local contributions, respectively. This treats the soft-wall non-locally and is consistent with the non-local nature of the higher-order diagrams Ω_n^{n+1}, with $n = 2, 3, \ldots$, in the NL binding potential functional $W[\ell]$ which sum to give the hard-wall restriction. Alternatively, one could omit the second term in (140) and add a contribution $c\Theta(-\ell)$ to (139). This treats the soft-wall contribution entirely locally, in the same fashion as Fisher and Huse [3]. However, these concerns are not of central importance for a number of reasons. Firstly, they play no part in regime I ($0 < \omega < 1/2$), where the short-distance behaviour of the local and non-local contributions to the binding potential are unimportant. If a stiffness-instability does not occur in this regime, it certainly does not occur when $\omega > 1/2$. Secondly, even when $\omega > 1/2$, it transpires that the direct contribution to the repulsion, determined by the renormalization of the first term in (140), is greater than the contribution arising from the renormalization of the soft-wall ($\propto c$). This is true regardless of how we treat the soft-wall repulsion (locally or non-locally) in the linear RG analysis. It is possible that, in the strongest fluctuation regime ($\omega > 2$), the linear RG predictions depend on the local or non-local treatment of the soft-wall. However, this regime is, strictly speaking, beyond the reach of the linear RG and will not be considered.

5.2. *The order of the phase transition*

The integrated RG flow equations allow us to draw several conclusions. We focus initially on the simplest regime $\omega < 1/2$, where the soft-wall term $\propto c$ can be dropped. As we shall soon demonstrate, most of our remarks remain valid for larger values of ω also.

5.2.1. Absence of a stiffness-instability. Firstly and most importantly, the two-body potential $U_t(x;\ell)$ and the corresponding NL contribution to the binding potential function $W_t^{\rm NL}(\ell)$ are always positive and hence represent a repulsive interfacial interaction with the wall. The bare critical wetting transition therefore cannot be fluctuation-induced first-order since this relies on the next-to-leading-order contribution to the renormalized potential function $W_t(\ell)$ becoming attractive. As remarked earlier, the FJ approximation to the bare interaction, $U_{\rm FJ}(x;\ell) \approx b_1 e^{-2\kappa\ell}(1-\kappa\ell(\nabla\ell)^2)\delta(\mathbf{x})$, is only valid for $\kappa\ell(\nabla\ell)^2 \ll 1$ and crucially gets the sign of the interaction wrong for larger wavevectors.

5.2.2. Weakened interfacial repulsion. Next, note that the width of the Gaussian determining the renormalized potential $U_t(x;\ell)$ depends on the distance x and is determined by the function $\Phi(x,t)$. Consider first the renormalization of the central value of the two-body potential. In the limit $x \to 0$, we have

$$\Phi(0^+, t) = t \quad (141)$$

leading to

$$U_t(0;\ell) = \frac{\kappa e^{4t}}{\sqrt{4\pi\omega t}} \int d\ell' U_0(0;\ell') e^{-\kappa^2(\ell-\ell')^2/4\omega t}. \quad (142)$$

The width of this convolution is identical to that appearing in the Fisher–Huse analysis describing the evolution of the local contribution. For fixed t, the function $\Phi(x,t)$ is bounded from above by t. Therefore, if we ignore the x dependence of this function and replace $\Phi(x,t)$ in (135) with t for all x, we overestimate the extent of the renormalization. In this case, we can integrate over the x coordinate in (138) and obtain the upper bound

$$\Delta W_t^{\rm NL}(\ell) < W_t^{\rm rep}(\ell;\omega) \quad (143)$$

where recall $W_t^{\rm rep}(\ell;\omega)$ is given by (21). Thus, the renormalized repulsion is smaller in the NL theory than in the CW theory. This means that the wetting film is thinner and also that the parallel correlation length is smaller than the corresponding predictions of the CW theory.

5.2.3. Mean-field as a lower bound. In the limit of large separation x, the renormalization of the two-body potential is controlled by

$$\Phi(\infty, t) = \frac{t}{2}. \tag{144}$$

Thus, we can anticipate that, by replacing $\Phi(x, t)$ in (135) with $t/2$, we underestimate the extent of the renormalization for all finite x. This leads to the lower bound

$$\Delta W_t^{\mathrm{NL}}(\ell) > W_t^{\mathrm{rep}}(\ell; \omega/2) \tag{145}$$

where the RHS is the CW result for the repulsion evaluated at half the value of the wetting parameter. In fact, this intuition can be rigorised by noting that $\Phi(x, t)$ is bounded from below by $t/2 - 0.2$ for $\Lambda x e^t > 1$. The right-hand side of (145) is readily evaluated and, indeed, can be read directly from the analysis of Fisher and Huse. We find

$$W_t^{\mathrm{rep}}(\ell; \omega/2) \approx b_1 \mathrm{e}^{2t+2\omega t-2\kappa\ell} \tag{146}$$

which is valid for $\omega < 1$. Notice that the condition on the bound now is not $\omega < 1/2$ because the bound itself is determined by half the value of the wetting parameter. The demarkation into regimes I ($0 < \omega < 1/2$), II ($1/2 < \omega < 2$) and III ($\omega > 2$) is appropriate for the asymptotic critical behaviour, but cross-over effects are not so clear-cut.

This lower bound on the repulsion has a remarkable physical interpretation since it leads to mean-field-like criticality even thought the value of the wetting parameter ω is non-zero. This follows from using (146) together with the leading-order term $V_t(\ell) \approx a\mathrm{e}^{2t+\omega t-\kappa\ell}$ (which is valid for $\omega < 2$). The usual matching condition then leads only to *mean-field critical behaviour* described by the critical exponents $\alpha_s = 0$ and $\nu_\parallel = 1$. Non-universality does not emerge in this lower bound even though the renormalized attraction and repulsion are both altered by fluctuation effects. We can therefore be certain that observables such as the equilibrium film thickness, the excess free-energy, and the parallel correlation length take values which all lie between the predictions of mean-field theory and the non-universality of the CW model.

5.2.4. Non-universality. A more telling lower bound can be obtained by considering the properties of $\Phi(x, t)$ in more detail. The width of the Gaussian determining the renormalized two-body interaction depends on the distance x. Equivalently, one may define a function $\omega(x)$ by

$$\omega(x) = \omega \frac{\Phi(x\mathrm{e}^{-t^*}, t^*)}{t^*} \tag{147}$$

which allows us to write the renormalized NL binding potential function as

$$\Delta W_{t^*}^{\mathrm{NL}}(\ell) = \kappa \mathrm{e}^{2t^*} \int\int \mathrm{d}\mathbf{x}\, \mathrm{d}\ell' U_0(x; \ell') \frac{\mathrm{e}^{-\kappa^2(\ell-\ell')^2/4\omega(x)t^*}}{\sqrt{4\pi\omega(x)t^*}}. \tag{148}$$

Thus, $\omega(x)$ clearly interpolates between the upper and lower bounds controlling the renormalization at $x = 0$ and $x = \infty$, respectively. Provided $x > 1/\Lambda$ and $x\Lambda \mathrm{e}^{-t^*} \ll 1$, a straightforward calculation shows

$$\omega(x) \approx \omega - \frac{\omega}{2} \frac{\ln \Lambda x}{t^*} + \cdots. \tag{149}$$

It is this value of the wetting parameter which determines the width of the Gaussian convolution with the bare two-body interaction for fixed x. Since at the matching point $\mathrm{e}^{t^*} \approx \xi_\parallel$ (by definition), we can write

$$\omega(x) \approx \omega - \omega \frac{\ln \sqrt{\Lambda x}}{\ln \Lambda \xi_\parallel} + \cdots. \tag{150}$$

This is strikingly similar to the formula for the effective value of the wetting parameter ω_{eff} which emerged in the Ginzburg criterion.

Now, note that $U_0(x; \ell') \approx \mathrm{e}^{-2\kappa\ell'\sqrt{1+(x/\ell')^2}}$, implying the bare two-body interaction is negligible compared to its central value for all separations $x \gg \ell'$. Therefore, if we replace $\omega(x)$ with $\omega(\lambda)$, where the distance λ scales faster than ℓ', then we will certainly be underestimating the renormalized repulsion. This can be achieved by writing $\Lambda\lambda \sim (\Lambda\ell')^\delta$ with exponent $\delta > 1$. In addition, since, at matching, the saddle point value of ℓ' is less than the equilibrium film thickness $\langle\ell\rangle$, we can strength the lower bound to

$$\Delta W_{t^*}^{\mathrm{NL}}(\ell) > W_{t^*}^{\mathrm{rep}}(\ell; \omega_\delta) \tag{151}$$

where

$$\omega_\delta = \omega - \omega\delta \frac{\ln \sqrt{\Lambda\langle\ell\rangle}}{\ln \Lambda\xi_\parallel} + \cdots \tag{152}$$

and is valid for $\delta > 1$ and large values of $\langle\ell\rangle$ and $\xi_\parallel$. Now, as $T \to T_{\mathrm{w}}$, both $\langle\ell\rangle$ and $\xi_\parallel$ diverge but always such that $\xi_\parallel \gg \langle\ell\rangle$. Thus, as we approach the (reduced) asymptotic critical regime, $\omega_\delta \to \omega$. Taken together with the upper bound, this shows that the asymptotic critical behaviour is non-universal and its leading order exactly the same as that predicted by the original CW model.

5.2.5. The effective value of the wetting parameter. The above lower bound fails for $\delta = 1$, since we can no longer be sure we are underestimating the fluctuation effects by replacing x with $\langle\ell\rangle$ in (150). In this case, we identify $\omega_\delta \equiv \omega(\langle\ell\rangle)$ where, from (150),

$$\omega(\langle\ell\rangle) = \omega - \omega \frac{\ln \sqrt{\Lambda\langle\ell\rangle}}{\ln \Lambda\xi_\parallel} \cdots. \tag{153}$$

It is notable that this is the same as the expression for the effective value of the wetting parameter ω_{eff} determining the reduced Ginzburg criterion, except that all length-scales now take their equilibrium as opposed to their mean-field values. It follows that the renormalized repulsion within the NL theory behaves as

$$\Delta W_{t^*}^{\mathrm{NL}}(\ell) \approx W_{t^*}^{\mathrm{rep}}(\ell; \omega_{\mathrm{eff}}) \tag{154}$$

at least for small values of ω, typical of regime I. Consequently, the effective wetting parameter ω_{eff} also helps quantify the slower approach to the asymptotic critical regime arising from the weaker renormalized repulsion.

It is notable that, in regime I (and also in regime II), the wetting temperature is not altered by fluctuations and occurs when $a = 0$. Thus, if we sit exactly at the critical wetting temperature T_w and approach the transition along the critical isotherm $h \to 0^-$, the only contributions to the binding potential are a trivial local term $\bar{h}\ell$ and the non-local repulsion. The local term renormalizes in a simple manner $\bar{h}\ell \to \bar{h}\ell e^{2t}$ and does not depend on the wetting parameter. Thus, the value of the wetting parameter measured along the critical isotherm, which appears in thermodynamic observables, arises solely from the non-local repulsion. This implies, for example, that the surface magnetization contains a singular term $m_1^{\text{sing}} \approx |h|^{1-1/2\nu_\parallel(\omega_{\text{eff}})}$ [9] and is determined by the lower (effective) value of the wetting parameter which characterizes the weaker repulsion of NL model. This is of direct relevance to the interpretation of the Ising model simulations which extracted critical singularities along this thermodynamic path.

The above arguments rely on the renormalization of the direct (local) attraction and direct (non-local) repulsion and ignores any contribution from the hard-wall proportional to c in (140). However, much of the above analysis goes through even when $\omega > 1/2$ where the hard-wall term is potentially important. Here, we address three pertinent questions: (A) is a stiffness-instability possible?, (B) is the repulsion weaker than predicted by CW theory?, and (C) is the cross-over to the (reduced) asymptotic critical regime controlled by a lower (effective) value of the wetting parameter?

The answer to the first question is certainly 'no'. Both the direct and hard-wall contributions to $\Delta W_{\text{NL}}(\ell)$ are positive, representing repulsive interactions. Hence, the wetting transition *cannot be driven first-order in any regime*. The answer to the second question is certainly 'yes'. The bound (143) applies equally to the direct and hard-wall contributions no matter what fluctuation regime we are in—all contributions to the renormalized repulsion are weaker in the NL theory compared to the CW model. There is, however, a subtle difference in the RG treatment of regime II in the CW and NL models.

Recall that, in the treatment of the CW model, the contributions from the direct and hard-wall repulsions are similar for $\omega > 1/2$. This is because the value of ℓ' which maximizes the integrand in (21) occurs when $\ell' = 0$, which is no longer the case in the NL theory due to the explicit dependence on position x. That is, for fixed x, we must consider what value of ℓ' maximizes the integrand in (148). A simple calculation shows that this is determined approximately from the solution of

$$\frac{2\omega\ell^2}{(\ell-\ell')^2} - \frac{x^2}{4\ell'^2} = 1 \tag{155}$$

where we have assumed that $\omega \geqslant 1/2$. For $x \ll \ell$, this implies $\ell' \approx \sqrt{2\omega - 1}(x/2)$, while, for $x \gg \ell$, we have $\ell' \approx \ell$. In other words, the renormalized direct repulsion is determined by the short-distance behaviour, only exactly at $x = 0$. For all finite x, the renormalized potential $U_t(x;\ell)$ is determined by fluctuations which do not take the interface all the way to the wall. The renormalized direct repulsion is greater than the renormalized hard-wall repulsion even for $\omega > 1/2$.

The last question is the most difficult one to answer. Provided $\omega < 1$, the lower bound on repulsion is still given by the expression (146). The hard-wall only changes this lower bound for $\omega > 1$. This is not something that need concern us for Ising-like systems where the physical value of $\omega \approx 0.8$. Thus, the critical behaviour must lie between the predictions of mean-field theory and the CW model, even allowing for a hard-wall term. The second-lower bound (151) also applies to both direct and hard-wall contributions and shows that the asymptotic critical regimes fall into the same categories predicted by Brezin *et al* [2]. What is more difficult to do, however, is to quantify the slower approach to the critical regime induced by non-locality. There are several reason for this. Firstly, even if the ultimate asymptotic critical behaviour belongs to regime II ($1/2 < \omega < 2$), the effective value of the wetting parameter for a given wetting film thickness might be less than 1/2. Indeed, our numerical results obtained from simulations of the NL model reveal precisely this. Secondly, we really do not know how reliable the linear RG is for assessing such a difficult question as the approach to non-universality in a regime where the hard-wall is important. Fortunately, our numerical results based on Monte Carlo simulation of the NL model reveal that the cross-over behaviour is rather well described by an effective value of the wetting parameter which emerges directly from the Ginzburg criterion and the second-lower bound obtained above, even for $\omega = 0.8$. We finish this section by showing how such an effective wetting parameter emerges from a simplified version of the RG.

5.3. *Interpretation as an effective cut-off*

There is an alternative and rather simple way of interpreting the impact of non-locality on fluctuation effects. Recall that the CW approximation to the two-body interfacial repulsion, $\mathcal{S}_{\text{CW}}(q) = 1$, is only valid for wavenumbers $q < 1/\xi_{\text{NL}}$. At higher wavenumbers, the repulsion is strongly suppressed. This suggests that the binding potential functional $W_{\text{NL}}[\ell]$ in (38) can be approximated by the local expression

$$W_{\text{NL}}[\ell] \approx a\int^{\Lambda} d\mathbf{x}\, e^{-\kappa\ell} + b_1\int^{\Lambda_{\text{NL}}} d\mathbf{x}\, e^{-2\kappa\ell} + \cdots \tag{156}$$

where, as indicated, we have introduced an effective momentum cut-off Λ_{NL} for the repulsion. This is similar to the discussion concerning the modification to the Ginzburg criterion where we set $\Lambda_{\text{NL}} \sim 1/\hat{\xi}_{\text{NL}}$. However, this procedure is not appropriate here since we do not wish to assume any mean-field-like behaviour. Instead, we can use $\Lambda_{\text{NL}} \approx \sqrt{\kappa/\ell_0}$ where, following (43) and (47), $\ell_0 = \int d\mathbf{x}\, \ell(\mathbf{x})/A$ is the mean interfacial height. We also impose the same wavevector restriction $q < \Lambda_{\text{NL}}$ on the approximate treatment of the hard-wall. The presence of a smoothed interfacial height ℓ_0 in the binding potential functional is reminiscent of weighted densities appearing in non-local density-functional theories of confined fluids [52], and is the simplest means of adapting the CW model to allow for the dampening effect of fluctuations on the repulsion. This approximate approach represents the limit to which one may apply local interfacial models to the three-dimensional critical wetting problem. The cut-off for the attractive term remains $\Lambda \approx \kappa$.

Apart from the change in the cut-off, expression (156) has the same form as the original CW theory. It is straightforward to modify the linear RG analysis of Fisher and Huse [3] to account for two distinct cut-offs by curtailing the RG flow of the repulsion before that of the attraction. At the matching point, this identifies $\ell_0 = \langle\ell\rangle$ and shows that the renormalization of the repulsion is determined by a reduced value of the wetting parameter. We omit these details because the analysis is even simpler to understand from the perspective of the RG scheme used by Brezin *et al* [2]. In their approach, one constructs an effective potential $W_{\rm eff}(\ell)$ by convoluting each term in the bare potential with a Gaussian

$$W_{\rm eff}(\ell) = \frac{1}{\sqrt{2\pi}\xi_\perp}\int_{-\infty}^{\infty} {\rm d}\ell' W_0(\ell'){\rm e}^{-(\ell-\ell')^2/2\xi_\perp^2} \qquad (157)$$

where

$$\kappa^2\xi_\perp^2 = \omega\ln(1+\Lambda^2\xi_\parallel^2) \qquad (158)$$

identifies the roughness. Then, one analyses the effective potential in a self-consistent manner and determines the correlation length according to $\xi_\parallel^{-2} = W''_{\rm eff}(\langle\ell\rangle)/\Sigma$.

For the binding potential functional (156), one sees immediately that the repulsive term renormalizes similarly to (157) but with $\xi_\perp$ replaced with a smaller width $w_\perp$, satisfying

$$\kappa^2 w_\perp^2 = \omega\ln(1+\Lambda_{\rm NL}^2\xi_\parallel^2) \qquad (159)$$

where $\Lambda_{\rm NL} \approx \sqrt{\kappa/\langle\ell\rangle}$. This is equivalent to saying that both the direct and hard-wall repulsions are determined by an effective wetting parameter

$$\omega_{\rm eff} = \omega\frac{\ln(1+\Lambda_{\rm NL}^2\xi_\parallel^2)}{\ln(1+\Lambda^2\xi_\parallel^2)}. \qquad (160)$$

This is the same as the equation emerging from the Ginzburg criterion analysis, (116), except all the quantities now take their equilibrium values as opposed to their mean-field values. Provided $\kappa\langle\ell\rangle \gg 1$, we may express this solely in terms of the wetting film thickness, which leads us to

$$\omega_{\rm eff} = \omega - c(\omega)\frac{\ln\kappa\langle\ell\rangle}{\kappa\langle\ell\rangle} + \cdots \qquad (161)$$

where the dimensionless coefficient c depends on the regime. For $0 < \omega < 1/2$, we have $c(\omega) = \omega(1+2\omega)/2$, while, for $\omega > 1/2$, we find $c(\omega) = \sqrt{2\omega^3}$. Thus, the effective value only approaches its true asymptotic value very slowly as the wetting film grows. In writing (161), we have assumed, for simplicity, that $\omega_{\rm eff}$ also falls into the same regime as ω. This may not be the case for thin wetting layers, or near a regime borderline.

If one wished, one could include a position-dependent stiffness in the above (amended) local interfacial description. Treated correctly, such a term no longer alters the order of the phase transition. The FJ model is equivalent to the approximation $\mathcal{S}_{\rm FJ}(q) \approx 1 - q^2\xi_{\rm NL}^2$ and is only valid for sufficiently long wavelengths, $q < \Lambda_{\rm NL}$. Thus, the troublesome next-to-leading-order position-dependent stiffness term appearing in the FJ Hamiltonian (25) should be written

$$-\kappa b_1\int^{\Lambda_{\rm NL}} {\rm d}\mathbf{x}\,\ell{\rm e}^{-2\kappa\ell}(\nabla\ell)^2 \qquad (162)$$

and is subject necessarily to the same wavevector restriction imposed on the direct repulsion in the local binding potential function (156). The mixing of the flow equations is now equivalent to a modified bare binding potential given by

$$\bar{W}_0(\ell) = \bar{a}{\rm e}^{-\kappa\ell} + b_1(1-\omega\xi\ell\Lambda_{\rm NL}^2){\rm e}^{-2\kappa\ell}. \qquad (163)$$

If the momentum cut-off were taken to be $\Lambda \sim \kappa$, then we would indeed have a stiffness-instability as predicted by Fisher and Jin. However, the corrected value of the cut-off cancels the problematic polynomial dependence on the film thickness. Consequently, there is no change in the sign of the next-to-leading-order exponential and, therefore, no stiffness-instability. A very similar flaw is present in generalizations of the FJ model which allow for coupling between interfacial fluctuations and those in the order-parameter near the wall [20, 21].

6. Numerical simulation of the interfacial models

In order to check the above predictions, we perform Monte Carlo simulations of discretized versions of the CW, FJ and NL Hamiltonians. Our approach follows closely that of Gompper and Kroll [42], whose simulations of the CW Hamiltonian confirmed convincingly the RG predictions of non-universality for this model. Thus, following [42], we discretize space by introducing an $L \times L$ square lattice of spacing σ with periodic boundary conditions in the directions parallel to the surface, but treating the interfacial position height as a continuous variable. The length-scale σ determines the value of the high momentum cut-off $\Lambda \approx \pi/\sigma$, and is taken to be an appropriate multiple of the bulk correlation length ξ_β. In each Monte Carlo step, we choose a lattice site i at random and increment the interfacial height $\ell_{\rm i} \equiv \ell(\mathbf{x}_i)$ by a random number which follows a uniform probability distribution on the interval $[-\Delta\ell, \Delta\ell]$, and use the usual Metropolis algorithm to accept or reject the new configuration [53]. The parameter $\Delta\ell$ is chosen so that approximately 40%–50% of the Monte Carlo attempted configurations are accepted. In order to assess finite-size effects, we use $L = 101$ and 201. Averages are evaluated over $10^6/10^7$ Monte Carlo steps per site, after an equilibration period of about $10^5/10^6$ Monte Carlo steps per site for $L = 101/201$.

Our simulations of the interfacial Hamiltonians are performed along the mean-field critical wetting isotherm, for which the coefficients in the binding potential (functional) satisfy $a = b_2 = 0$, and the bulk ordering field $\bar{h} \to 0$. For this choice of parameters, and written in terms of ω, the continuum CW model (5) is given explicitly by

$$H_{\rm CW}[\ell] = \int {\rm d}\mathbf{x}\left\{\frac{k_{\rm B}T\kappa^2}{8\pi\omega}(\nabla\ell)^2 + \bar{h}\ell + b_1{\rm e}^{-2\kappa\ell}\right\} \qquad (164)$$

with its discretized version

$$H^*_{\rm CW}(\{\ell_{\rm i}\}) = \frac{\kappa^2 k_{\rm B}T}{16\pi\omega}\sum_{i,n}(\ell_{\rm i}-\ell_{i+n})^2 + \sigma^2\sum_i\left(\bar{h}\ell_{\rm i}+b_1{\rm e}^{-2\kappa\ell_{\rm i}}\right) \quad (165)$$

where the sum over n is restricted to the nearest neighbours of the site i, denoted by $i+n$. In this discretization, we have used the standard approximation $(\nabla\ell(\mathbf{x}_i))^2 \approx \frac{1}{2\sigma^2}\sum_n(\ell_{\rm i}-\ell_{i+n})^2$ for the square-gradient term.

The continuum and discretized versions of the FJ model are

$$H_{\rm FJ}[\ell] = \int {\rm d}\mathbf{x}\left\{\left(\frac{k_{\rm B}T\kappa^2}{8\pi\omega} - b_1\kappa\ell{\rm e}^{-2\kappa\ell}\right) \times (\nabla\ell)^2 + \bar{h}\ell + b_1{\rm e}^{-2\kappa\ell}\right\} \quad (166)$$

and

$$H^*_{\rm FJ}(\{\ell_{\rm i}\}) = \sum_{i,n}\left[\frac{\kappa^2 k_{\rm B}T}{16\pi\omega} - \kappa\ell_{\rm i}b_1{\rm e}^{-2\kappa\ell_{\rm i}}\right](\ell_{\rm i}-\ell_{i+n})^2 + \sigma^2\sum_i\left(\bar{h}\ell_{\rm i}+b_1{\rm e}^{-2\kappa\ell_{\rm i}}\right) \quad (167)$$

both of which contain a position-dependent stiffness-coefficient.

Finally, the continuum and discretized versions of the NL model are

$$H_{\rm NL}[\ell] = \int {\rm d}\mathbf{x}\left\{\frac{k_{\rm B}T\kappa^2}{8\pi\omega}(\nabla\ell)^2 + \bar{h}\ell\right\} + \int\int {\rm d}\mathbf{x}_1\,{\rm d}\mathbf{x}_2 U\left(x_{12};\bar{\ell}\right) \quad (168)$$

and

$$H^*_{\rm NL}(\{\ell_{\rm i}\}) = \frac{\kappa^2 k_{\rm B}T}{16\pi\omega}\sum_{i,n}(\ell_{\rm i}-\ell_{i+n})^2 + \sigma^2\sum_i\left(\bar{h}\ell_{\rm i}\right) + \sigma^4\sum_{i,j}U\left(x_{ij};\bar{\ell}\right) \quad (169)$$

where the mean-geometric heights are $\bar{\ell} = (\ell(\mathbf{x}_1)+\ell(\mathbf{x}_2))/2$ and $\bar{\ell} = (\ell_{\rm i}+\ell_j)/2$ for the continuum and discretized versions, respectively. The two-body interaction $U(x;\ell)$ is calculated by numerical integration of (42), and is set to zero for $x > R_{\text{cut-off}} = 4\sigma$, which is appropriate provided $\kappa\langle\ell\rangle < 10$.

Before we discuss the simulation results, a few remarks are in order. In writing the NL model, we have made the usual square-gradient approximation to the full-area term $\sqrt{1+(\nabla\ell)^2} \approx 1+(\nabla\ell)^2/2$, since this approximation is also inherent in the CW and FJ models. However, we have also performed simulations of the full-area description of the NL model, which does not assume the gradient expansion. We found that the larger the value of the discretization parameter σ, the closer the simulation results obtained between the square-gradient and the full-area versions of the NL model. This is entirely in keeping with elementary physical considerations, since the typical value of the interfacial height gradient is of order $|\nabla\ell| \sim \xi_\beta/\sigma$, implying that we can safely neglect terms $\mathcal{O}((\nabla\ell)^4)$ and higher-order terms for large $\kappa\sigma$.

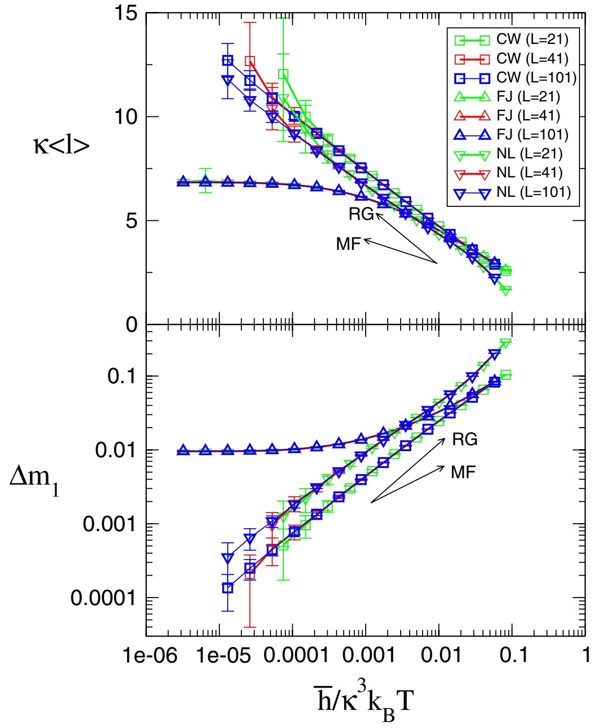

Figure 5. Plot of the mean wetting layer thickness $\langle\ell\rangle$, measured in units of the bulk correlation length, and surface magnetization operator $\Delta m_1 = \langle{\rm e}^{-\kappa\ell}\rangle$ versus reduced (dimensionless) bulk field h obtained by computer simulations of the CW FJ, and NL models for $\omega = 0.8$, $a = b_2 = 0$, and $b_1/\kappa^2 k_{\rm B}T = 2.5$. For the FJ model, the wetting layer thickness saturates, consistent with a first-order phase transition, while both the CW and NL models give critical wetting. The approach to the asymptotic critical regime for the NL model is considerably slower than for the CW model.

For the choice $\sigma = 3.1623\kappa^{-1}$, the numerical results of the two models are similar and only results for the square-gradient approximation (169) are reported. We also choose $\omega = 0.8$ and $b_1 = 2.5\kappa^2 k_{\rm B}T$, which are reasonable Ising-like parameters. We anticipate the critical wetting phase boundary remains mean-field ($a = 0$) for the CW and NL theories [3], whilst the FJ exhibits a first-order transition at a higher temperature [16].

Figure 5 describes the behaviour of the mean wetting layer thickness $\langle l\rangle$ and the surface magnetization-like operator $\Delta m_1 = \langle{\rm e}^{-\kappa l}\rangle$ along the mean-field critical wetting isotherm $a = 0$, $\bar{h} \to 0$. The FJ model clearly describes partial wetting in this limit, consistent with a fluctuation-induced first-order transition. On the other hand, the CW and NL models are qualitatively similar, showing continuous wetting. The growth of the film thickness conforms to the anticipated logarithmic divergence $\kappa\langle l\rangle \sim -\ln\bar{h}$ even for moderately thick wetting layers. However, the surface magnetization shows a much larger preasymptotic critical regime. The asymptotic non-universal behaviour $\Delta m_1 \sim \bar{h}^{1-1/2\nu_\parallel}$, with $\nu_\parallel(\omega) = (\sqrt{2}-\sqrt{\omega})^{-2}$ is *not observed* even for thick wetting layers, $\kappa\langle l\rangle \sim 10$, and very large lattice sizes $\kappa L \sim 300$. This is strongly suggesting that, unless Ising model simulations of wetting are conducted in very large systems, significant deviations from mean-field behaviour will not be observed. Nevertheless, mean-field theory will ultimately breakdown.

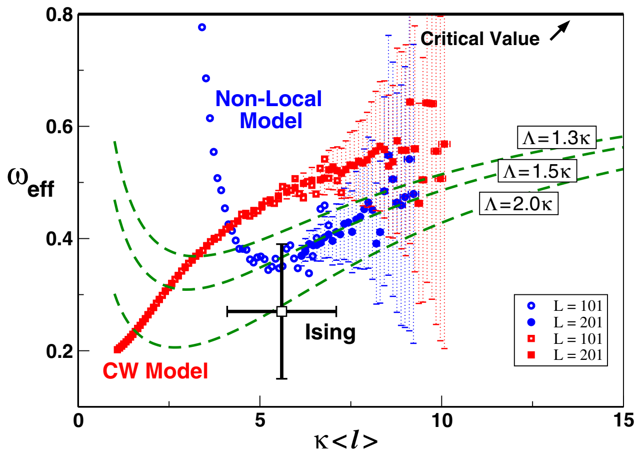

Figure 6. Effective value of the wetting parameter as a function of the equilibrium wetting thickness $\kappa\langle\ell\rangle$. Simulations of the discretized local (squares) and non-local (circles) interfacial models were performed on an $L \times L$ grid (of unit length σ). The dashed lines are predictions of the continuum approximation (170) for different values of the momentum cut-off Λ. The value of $\omega_{\rm fit}$ obtained from Ising model simulations [13] is also shown (square).

In figure 6, we plot the effective value of the wetting parameter $\omega_{\rm eff}$ versus the film thickness $\kappa\langle\ell\rangle$ as obtained from the simulation data of the CW and NL models. In the simulation studies of the interfacial models, $\omega_{\rm eff}$ has been extracted from the singularity of the surface magnetization $\Delta m_1 \approx \bar{h}^{1-1/2\nu_\parallel(\omega_{\rm eff})}$, along the critical isotherm. This is more difficult for the Ising model, and we have used the estimate taken from the surface susceptibility critical amplitude [13]. As can be seen, the NL theory is in better agreement with the Ising model simulation result due to the slower cross-over. In addition to this, an intriguing feature of the simulation results of the NL model is the non-monotonic behaviour of $\omega_{\rm eff}$ with film thickness and the presence of a minimum when $\kappa\ell \approx 5$. Both these features are consistent with the theoretical expression (160), obtained from the RG and Ginzburg criterion analysis of the continuum NL Hamiltonian. Substituting $\Lambda_{\rm NL} \approx \sqrt{\kappa/\langle\ell\rangle}$ and $\kappa\ell \approx \sqrt{2\omega}\ln(\Lambda^2\xi_\parallel^2)$ leads to the approximate expression for the thickness dependence

$$\omega_{\rm eff}(\ell) \approx \omega\frac{\ln(1+(\kappa/\ell\Lambda^2){\rm e}^{\kappa\ell/\sqrt{2\omega}})}{\ln(1+{\rm e}^{\kappa\ell/\sqrt{2\omega}})}. \qquad (170)$$

Numerical plots of this result for different values of the momentum cut-off Λ are shown as dashed lines in figure 6. These are reasonably close to the simulation findings, being substantially lower than the asymptotic value $\omega = 0.8$, and also show the presence of a minimum value of approximately 0.3 when the film thickness is approximately 5 bulk correlation lengths. The non-monotonic behaviour of $\omega_{\rm eff}$ can also be inferred from the change of curvature in the plot of Δm_1 versus $\bar{h}$, shown in figure 5. Unfortunately, in the original Ising simulation studies, the regime where $\omega_{\rm eff}$ increases with decreasing film thickness corresponds to wetting layers less than 1 or 2 lattice spacings, for which a continuum description is doubtful. However, this limitation can be overcome in future simulations at temperatures closer to T_c, where the bulk correlation length is much larger.

7. Conclusions

In this paper, we have used a non-local interfacial Hamiltonian to revisit some problems in the theory of three-dimensional short-ranged wetting. The NL model contains an additional diverging length-scale, $\xi_{\rm NL}$, not present in the basic capillary-wave description of wetting, which, we believe, is the likely reason why Ising model simulations did not reveal the anticipated non-universality. As stressed at the beginning of our paper, the dampening effect of the two-body interfacial repulsion on critical singularities can already be seen in the mean-field correlations calculated for the LGW model and leads directly to the reduction in the size of the critical regime at critical wetting. If this is present in the LGW model, it is highly likely it is also present in the Ising model.

Of course, we have not solved either the full three-dimensional LGW or an Ising model description of wetting. The present continuum NL interfacial model is only valid for thick wetting films much greater than the bulk correlation length. It gives no description of physics related to volume exclusion and lattice effects, which would lead to layering phenomena and the roughening transition, for example. At the very least, we believe the NL model does two things: (1) it provides a better understanding of the limitations of the original CW and FJ models of wetting, and highlights the importance of two-body interfacial interactions, (2) in a wider context still, the diagrammatic expansion of the binding potential functional $W[\ell, \psi]$ provides a systematic basis for understanding how wetting films and liquid drops behave near shaped substrates.

We do not know if the present revision in the phenomenology of short-ranged wetting has implications for systems with long-ranged fluid–fluid forces. Henderson's exact sum-rule for $G_2(0, 0)$ is valid for quite arbitrary choices of fluid–fluid intermolecular potential, and analogous questions exists about how this is satisfied exactly by an interfacial Hamiltonian. In addition, recent density-matrix RG studies of critical wetting in a two-dimensional Ising model with marginal long-ranged substrate interactions did not reveal the anticipated non-universality predicted on the basis of the standard interfacial Hamiltonian [54]. Perhaps, this points to the presence of additional length-scales for wetting in systems with long-ranged forces. Finally, returning to the case of short-ranged forces, we have not yet been able to generalize the nonlinear RG analysis to account for two-body repulsive interactions. Although this would be welcome, it is overoptimistic to think this would give an analytic insight into the slower approach to the critical regime. Rather, it would be interesting to understand if non-locality alters the fixed-point analysis pertinent to the strong-fluctuation regime of critical wetting away from $d = 3$, and also the bifurcation mechanism as one approaches the upper critical dimension [41].

Acknowledgments

AOP and JMR-E are very grateful to Dr A Lazarides for discussions considering the renormalization group analysis of the non-local model. NRB thanks Dr M Tasinkevych for help with the simulations. JMR-E, NRB and CR acknowledge support from grants No. ENE2007-6804-C03-02 (Ministerio de Educación y Ciencia) and P06-FQM-01869 (Junta de Andalucía), the Portuguese FCT, and grants MOSAICO (Ministerio de Educación y Ciencia) and MOSSNOHO (Comunidad de Madrid), respectively.

References

[1] For reviews of wetting, see Dietrich S 1988 *Phase Transitions and Critical Phenomena* vol 12, ed C Domb and J L Lebowitz (New York: Academic)
Or Schick M 1990 *Liquids at Interfaces* ed J Charvolin, J F Joanny and J Zinn-Justin (Amsterdam: Elsevier) p 3364
[2] Brézin E, Halperin B I and Leibler S 1983 *Phys. Rev. Lett.* **50** 1387
[3] Fisher D S and Huse D A 1985 *Phys. Rev.* B **32** 247
[4] Lipowsky R, Kroll D M and Zia R K P 1983 *Phys. Rev.* B **27** 4499
[5] Sullivan D E and Telo da Gama M M 1986 *Fluid Interfacial Phenomena* ed C A Croxton (London: Wiley) p 45
[6] Nakanishi H and Fisher M E 1982 *Phys. Rev. Lett.* **49** 1565
[7] Fisher M E and Wen H 1992 *Phys. Rev. Lett.* **68** 3654
[8] Evans R, Hoyle D C and Parry A O 1992 *Phys. Rev.* A **45** 3823
[9] Binder K, Landau D P and Kroll D M 1986 *Phys. Rev. Lett.* **56** 2272
[10] Binder K and Landau D P 1988 *Phys. Rev.* B **37** 1745
[11] Binder K, Landau D P and Wansleben S 1989 *Phys. Rev.* B **40** 6979
[12] Binder K, Landau D P and Müller M 2003 *J. Stat. Phys.* **110** 1411
[13] Parry A O, Evans R and Binder K 1991 *Phys. Rev.* B **43** 11535
[14] Fisher M E and Jin A J 1991 *Phys. Rev.* B **44** 1430
[15] Jin A J and Fisher M E 1993 *Phys. Rev.* B **47** 7365
[16] Fisher M E and Jin A J 1992 *Phys. Rev. Lett.* **69** 792
[17] Jin A J and Fisher M E 1993 *Phys. Rev.* B **48** 1897
[18] Fisher M E, Jin A J and Parry A O 1994 *Bunsenges. Phys. Chem.* **98** 357
[19] Boulter C J 2001 private communication
[20] Boulter C J and Parry A O 1995 *Phys. Rev. Lett.* **74** 3403
Parry A O and Boulter C J 1995 *Physica* A **218** 77
Boulter C J and Parry A O 1995 *Physica* A **218** 109
[21] Swain P S and Parry A O 1997 *Europhys. Lett.* **37** 207
Parry A O and Swain P S 1998 *Physica* A **250** 167
[22] Parry A O, Rascón C, Bernardino N R and Romero-Enrique J M 2006 *J. Phys.: Condens. Matter* **18** 6433
[23] Parry A O, Rascón C, Bernardino N R and Romero-Enrique J M 2007 *J. Phys.: Condens. Matter* **19** 416105
[24] Parry A O, Greenall J M and Wood A J 2002 *J. Phys.: Condens. Matter* **24** 1169
[25] Parry A O, Wood A J and Rascón C 2001 *J. Phys.: Condens. Matter* **13** 4591
[26] Rascón C and Parry A O 2005 *Phys. Rev. Lett.* **94** 096103
[27] Parry A O, Greenall M G and Romero-Enrique J M 2003 *Phys. Rev. Lett.* **90** 046101
[28] Greenall M G, Parry A O and Romero-Enrique J M 2004 *J. Phys.: Condens. Matter* **16** 2515
[29] Kac M 1966 *Am. Math. Monthly* **73** 1
[30] Balian R and Bloch C 1970 *Ann. Phys.* **60** 401
[31] Adagideli I, Sheehy D E and Goldbart P M 2002 *Int. J. Mod. Phys.* **16** 1381
[32] Parry A O, Romero-Enrique J M and Lazarides A 2004 *Phys. Rev. Lett.* **93** 086104
[33] Parry A O, Rascón C, Bernardino N R and Romero-Enrique J M 2008 *Phys. Rev. Lett.* **100** 136105
[34] Henderson J R and van Swol F 1985 *Mol. Phys.* **56** 1313
See also Henderson J R 1992 *Fundamentals of Inhomogeneous Fluids* ed D Henderson (New York: Dekker) chapter 2
[35] Mikheev L V and Weeks J D 1991 *Physica* A **177** 495
[36] Parry A O and Evans R 1988 *Mol. Phys.* **65** 455
Parry A O and Evans R 1993 *Mol. Phys.* **78** 1527
[37] Cahn J W 1977 *J. Chem. Phys.* **66** 3667
[38] Ebner C and Saam W F 1977 *Phys. Rev. Lett.* **38** 1486–9
[39] Fisher D S, Fisher M P A and Weeks G D 1982 *Phys. Rev. Lett.* **48** 369
[40] Forgacs G, Lipowsky R and Nieuwenhuizen Th M 1991 *Phase Transitions and Critical Phenomena* vol 14, ed C Domb and J L Lebowitz (New York: Academic)
[41] Lipowsky R and Fisher M E 1986 *Phys. Rev. Lett.* **57** 2411
Lipowsky R and Fisher M E 1987 *Phys. Rev.* B **36** 2126
[42] Gompper G and Kroll D M 1988 *Phys. Rev.* B **37** 3821
[43] Boulter C J 1997 *Phys. Rev. Lett.* **79** 1897
[44] Holyst R and Poniewierski A 1987 *Phys. Rev.* B **36** 5628
[45] Gelfand M P and Lipowsky R 1987 *Phys. Rev.* B **36** 8725
[46] Brézin E, Halperin B I and Leibler S 1983 *J. Physique* **44** 775
[47] Lipowsky R and Speth W 1983 *Phys. Rev.* B **28** 3983
[48] Parry A O and Boulter C J 1994 *J. Phys. A: Math. Gen.* **27** 1877
[49] Bernardino N R 2008 *PhD Thesis* Imperial College London, unpublished
[50] Halpin-Healy T and Brezin E 1987 *Phys. Rev. Lett.* **58** 1220
[51] Romero-Enrique J M, Lazarides A and Parry A O 2008 in preparation
[52] Evans R 1992 *Fundamentals of Inhomogeneous Fluids* ed D Henderson (New York: Dekker) chapter 1
[53] Landau D P and Binder K 2005 *A Guide to Monte Carlo Simulations in Statistical Physics* (Cambridge: Cambridge University Press)
[54] Drzewinski A, Parry A O and Szota K 2007 *Phys. Rev.* E **75** 041110